# **Introduction to Special Section: Photochemistry Experiment** in **BERLIOZ**

Andreas Volz-Thomas, Heiner Geiss, and Andreas Hofzumahaus Institut für Chemie und Dynamik der Geosphäre II, Forschungszentrum Jülich, Jülich, Germany

### Karl-Heinz Becker

Fachbereich 9, Physikalische Chemie, Bergische Universität Gesamthochschule Wuppertal, Wuppertal, Germany

Received 20 December 2001; revised 3 May 2002; accepted 12 June 2002; published 29 January 2003.

[1] PHOEBE was conducted during the Berlin Ozone Experiment (BERLIOZ) between 5 July and 7 August 1998 near the city of Berlin. It aimed at a quantitative understanding of the fast radical chemistry in rural and suburban air by simultaneous measurements of the major free radicals (OH, HO<sub>2</sub>, RO<sub>2</sub>, and NO<sub>3</sub>) and the chemical compounds and physical parameters that control the radical concentrations. Interpretation of the measurements involved models of different complexity. The methods deployed and the results are discussed in the subsequent publications of this special section. This paper outlines the aims of PHOEBE, describes the observational site at Pabstthum, and briefly summarizes the different measurements and instrument comparisons as well as the main results of the accompanying publications. *INDEX TERMS*: 0322 Atmospheric Composition and Structure: Constituent sources and sinks; 0345 Atmospheric Composition and Structure: Pollution—urban and regional (0305); 0394 Atmospheric Composition and Structure: Instruments and techniques; *KEYWORDS*: field campaign, free radicals, modeling, measurements, overview

Citation: Volz-Thomas, A., H. Geiss, A. Hofzumahaus, K.-H. Becker, Introduction to Special Section: Photochemistry Experiment in BERLIOZ, *J. Geophys. Res.*, 108(D4), 8252, doi:10.1029/2001JD002029, 2003.

#### 1. Introduction

[2] The transition region between urban and rural areas is important in understanding the fast photochemistry that leads to the build up of high concentrations of ozone and other photooxidants during so-called summer smog episodes. As is schematically outlined in reactions (R1)–(R5), hydrocarbon oxidation by hydroxyl radicals (OH) leads to formation of peroxy radicals (RO<sub>2</sub> and HO<sub>2</sub>), which oxidize NO to NO<sub>2</sub>, thereby regenerating the OH. Photolysis of the NO<sub>2</sub> then generates the oxygen atoms required to produce ozone [Chameides and Walker, 1973; Crutzen, 1979]. In this simplified view, the net effect of the radical chain in the presence of sufficient NO is that hydrocarbons are oxidized to carbonyl compounds (CARB, i.e., aldehydes and ketones) and O<sub>3</sub> [cf. Chameides et al., 1992]

$$(R1) \qquad R-H+OH+O_2+M \rightarrow RO_2+H_2O+M$$

$$(R2) \hspace{1cm} RO_2 + NO \rightarrow RO + NO_2$$

(R3) 
$$RO + O2 \rightarrow HO_2 + CARB$$

(R4) 
$$HO_2 + NO \rightarrow OH + NO_2$$

$$(2x) \qquad NO_2 + hn + O_2(+M) \rightarrow NO + O_3(+M)\lambda < 420 \ nm \label{eq:condition}$$
 (R5)

Copyright 2003 by the American Geophysical Union. 0148-0227/03/2001 JD002029

$$net: \qquad R-H+3\ O_2+hn \rightarrow CARB+2\ O_3+H_2O$$

Additional HO<sub>2</sub> is produced from the oxidation of CO:

$$(R6) \hspace{1cm} CO + OH + O_2(+M) \rightarrow CO_2 + HO_2(+M)$$

Production of OH radicals in the troposphere occurs mainly via photolysis of  $O_3$  ((R7) and (R8)) [Levy, 1971]

(R7) 
$$O_3 + h\nu \rightarrow O^1D + O_2 \qquad \lambda < 340 \text{ nm}$$

$$(R8) O1D + H2O \rightarrow 2 OH$$

Another potentially important source for OH, particularly in polluted air, is the photolysis of HONO which is formed either in the tail pipe of motor vehicles [Kessler and Platt, 1984] or upon emission in the atmosphere via heterogeneous reactions [Stockwell and Calvert, 1983].

(R9) 
$$HONO + h\nu \rightarrow OH + NO$$
  $\lambda < 405 \text{ nm}$ 

Since (R9) occurs at much longer wavelengths than (R8), it can produce OH during the early morning, when (R8) is still rather ineffective. Thereby, HONO photolysis is thought to provide an important trigger for photochemical smog formation in the urban and suburban environment [Harris et al., 1982; Platt, 1986; Jenkin et al., 1988; Calvert et al., 1994; Harrison et al., 1996; Volz-Thomas and Kolahgar, 2000]. Other sources of OH and peroxy radicals include the ozonolysis of olefinic VOC [cf. Paulson and Orlando, 1996; Kroll et al., 2001; Siese et al., 2001], and the reaction

of NO<sub>3</sub> radicals with organic compounds at night [Wayne et al., 1991; Mihelcic et al., 1993; Carslaw et al., 1997; Platt et al., 1990; Salisbury et al., 2001].

[3] During daytime, the concentration of OH and the production rate of ozone both depend on the UV flux (i.e., on the photolysis frequencies  $JO^1D$ ,  $JNO_2$ , JHONO, JHCHO, ...) and on the concentrations of  $H_2O$ ,  $O_3$ , CO,  $NO_x$ , and VOCs. The role of  $NO_x$  in the budgets of  $HO_x$  (OH and  $HO_2$ ) and ozone is ambivalent: At low  $NO_x$  concentrations, where recombination reactions of the peroxy radicals ((R10) + (R11)) constitute the major radical loss, NO controls the recycling of  $HO_x$  and is the rate limiting factor in ozone production [*Crutzen*, 1979].

(R10) 
$$HO_2 + HO_2 + M \rightarrow H_2O_2 + M$$

(R11) 
$$HO_2 + RO_2 + M \rightarrow ROOH + M$$

At high-NO<sub>x</sub> levels, radical losses by recombination of peroxy radicals become insignificant and HO<sub>2</sub> is almost completely recycled to OH in reaction (R4). Due to photolysis of the carbonyl compounds formed in reaction (R3), more radicals can be produced from the hydrocarbon oxidation mechanism than are initially consumed in (R1), depending on the VOC to NO<sub>x</sub> ratio and VOC reactivity [*Jeffries and Tonnesen*, 1994].

(R12) 
$$CARB + h\nu \rightarrow HO_2 + ....$$

This effect is counteracted by the reaction of OH with  $NO_2$ , which becomes the predominant sink of  $HO_x$  in the high- $NO_x$  regime and thus effectively limits the production of  $RO_2$  and  $HO_2$ .

(R13) 
$$NO_2 + OH + M \rightarrow HNO_3 + M$$

The net effect of  $NO_x$  on the radical balance and ozone formation depends on the  $NO/NO_2$  ratio, which is controlled by the photolysis rate of  $NO_2(R5)$  and by the concentrations of peroxy radicals and  $O_3$  via reactions (R2), (R4), and (R14).

$$(R14) NO_2 + O_3 \rightarrow NO + O_2$$

The radical chemistry in the high-NO<sub>x</sub> regime is further complicated by the photolysis of HONO (R9). Another complication in the understanding of the radical budget is the formation of alkyl nitrates and peroxyacyl nitrates, e.g., PAN. Alkyl nitrates are formed as by-products in (R2). The branching ratios tend to increase with the size of the organic rest and are higher for secondary and tertiary RO<sub>2</sub> [Atkinson et al., 1982, 1983, 1984, 1987; Becker and Wirtz, 1989]. The net effect is a decrease in the local ozone formation rate. Similarly, the production of peroxyacteyl nitrate (PAN) and its homologues by reaction of acylperoxy radicals with NO<sub>2</sub> (R15) removes peroxy radicals and NO<sub>x</sub> from the active pool. Thermal decomposition of the PAN compounds establishes equilibrium, but the net effect on the local radical balance depends on temperature and history of the air mass.

$$R - C(O) - OO + NO_2 + M \leftrightarrow R - C(O) - OO - NO_2 + M)$$
(R15)

- [4] Because of their short chemical lifetimes, free radicals (OH, HO<sub>2</sub>, and RO<sub>2</sub>) are largely decoupled from transport processes and can thus be investigated with zero dimensional chemistry models, provided that the chemical and physical parameters which control the local radical concentration, e.g., UV radiation, NO<sub>x</sub>, and VOC, are quantified. This is strictly the case only if the radicals and other parameters are measured with a time resolution given by the atmospheric lifetimes of the radicals, e.g., between less than 1 s for OH and a few seconds to minutes for the peroxy radicals. Until now this is an unsolved challenge for many atmospheric trace gases, in particular for hydrocarbons which in urban air can constitute of more than 100 different compounds [Ciccioli et al., 1992]. The interpretation of the radical measurements thus relies on assumptions about stationarity and homogeneity of the investigated air masses. These conditions are best achieved if the measurements are made at sufficient distance from sources or sinks and if the different measurements are made as close together as possible.
- [5] The fast photochemistry of the troposphere has been investigated by measurements of the concentrations of the free radicals (OH, HO2, and RO2) and of those chemical and physical parameters that are thought to control the radical concentrations. Besides airborne missions in the free troposphere [Brune et al., 1998; Mauldin et al., 1998; Wennberg et al., 1998], a strong emphasis has been on ground based studies, mostly in the planetary boundary layer (PBL) [cf. Perner et al., 1987; Platt et al., 1988; Eisele et al., 1994, 1996, 1997; Poppe et al., 1994; Cantrell et al., 1996, 1997; Armerding et al., 1997; Carpenter et al., 1997; McKeen et al., 1997; Mount and Williams, 1997; Penkett et al., 1997; Brandenburger et al., 1998; Holland et al., 1998; Jefferson et al., 1998; Carslaw et al., 1999; Ehhalt, 1999; Hauglustaine et al., 1999; Kanaya et al., 1999, 2000; Volz-Thomas and Kolahgar, 2000; Brauers et al., 2001; Carroll et al., 2001; Savage et al., 2001]. These field experiments qualitatively confirmed fundamental aspects of the free radical chemistry, such as the principal dependencies of OH on the ozone photolysis frequency JO<sup>1</sup>D and the concentration of NO<sub>x</sub>.
- [6] The quantitative comparison of measurements and models does not show a coherent picture. There is a general tendency of photochemical models to overestimate OH and peroxy radicals. Exceptions are the ALBATROSS, POP-CORN, and SCATE campaigns and the MLOPEX-2 campaign in spring, where modeled and measured OH were found to agree within the experimental uncertainties for clean air conditions [Eisele et al., 1996; Jefferson et al., 1998; Ehhalt, 1999; Brauers et al., 2001], and some campaigns conducted in forested areas (e.g., AEROBIC, PROPHET, and SLOPE) where OH was found to be significantly underestimated by the models [Volz-Thomas and Kolahgar, 2000; Carslaw et al., 2001; Creasey et al., 2001; Tan et al., 2001]. It is also noted that in some of the earlier studies, the comparison was somewhat limited by the lack of measurements for several trace gases that are of importance to OH formation or loss, e.g., part of the VOC. Very little information exists so far on the behavior of OH radicals in highly polluted atmospheres, except of the LAFRE campaign [George et al., 1999].
- [7] The PHOEBE campaign was planned to investigate the radical chemistry in an environment covering suburban

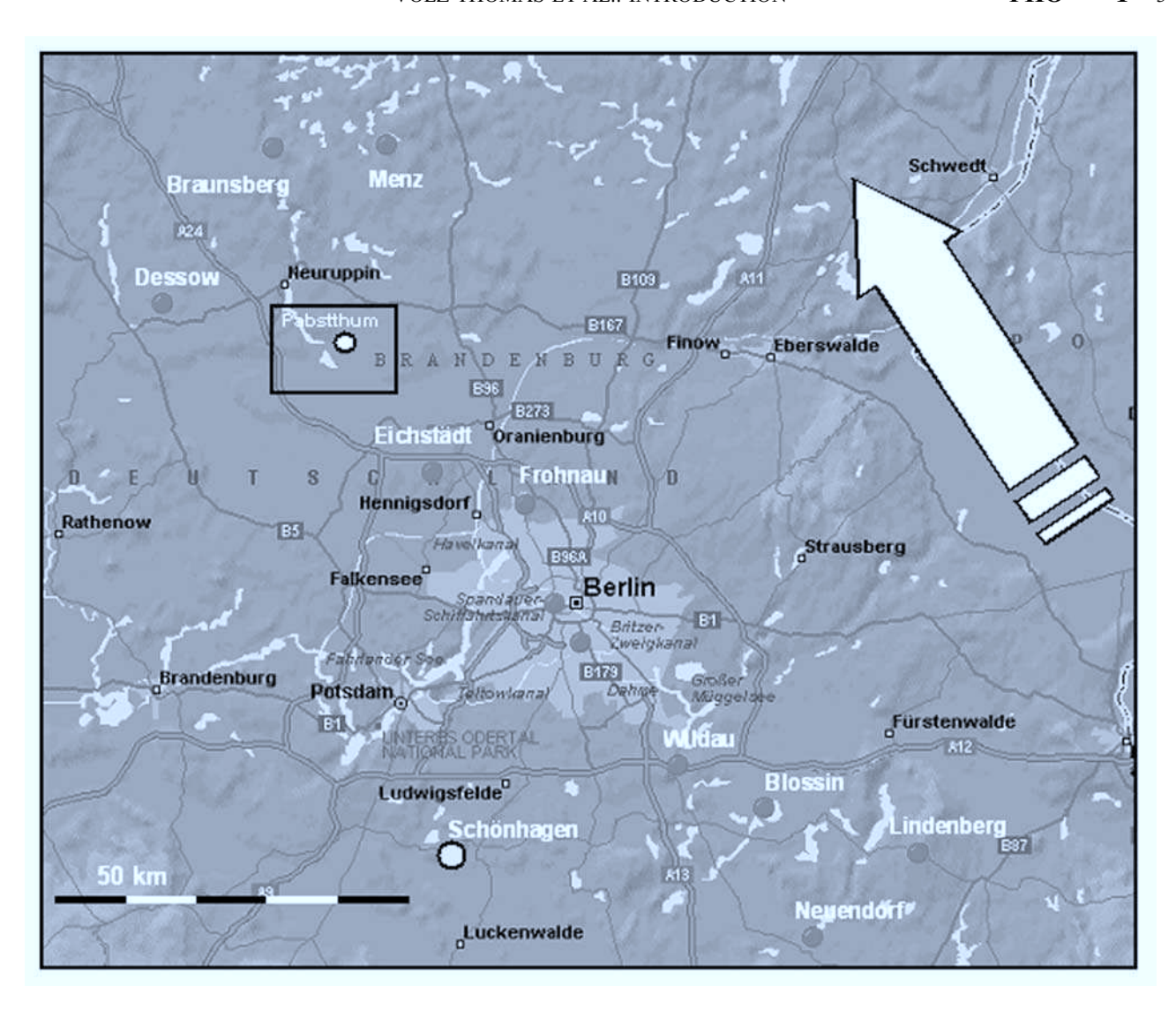


**Figure 1.** Map of the area around Berlin with the surface sites of BERLIOZ indicated by the red dots and the airfield Schönhagen by the yellow dot. The red lines denote motorways and major roads. See color version of this figure at back of this issue.

to rural conditions. It was a major activity of the Berlin Ozone Experiment (BERLIOZ) [Becker et al., 1999] which took place between 5 July and 7 August 1998 including 1 week for intercomparison and quality control of the different analytical instruments. The overall aim of the BERLIOZ was to analyze the transport and chemical processes responsible for photooxidant formation and the contribution of groups of precursor substances to the ozone formation in the Berlin area. For this purpose, many speciated hydrocarbons and carbonyl compounds, O<sub>3</sub>, PAN, NO, NO<sub>2</sub>, HNO<sub>2</sub>, HNO<sub>3</sub>, and NO<sub>3</sub> radicals (e.g., JNO<sub>2</sub> and JO<sup>1</sup>D) were measured at different ground based sites by in situ techniques, along with measurements of meteorological parameters and photolysis frequencies.

[8] A map of the area around Berlin with the BERLIOZ sites is shown in Figure 1. The sites had been lined up along an axis extending from ca. 70 km SE to 80 km NW of Berlin, according to the predicted main wind direction during episodes with large photochemical activity. In

addition to the surface sites, which were operational during the whole BERLIOZ period, 6 ozone LIDAR systems, 5 tethered balloons and 6 aircraft were deployed during intensive operational periods (IOPs). Some of the ground based measurements, i.e., carbonyl compounds, carboxylic acids, and the measurements of peroxy radicals by MIESR (see below) were also confined to the IOPs. The technical equipment, the achieved data, estimates of the precursor emissions and trace gas budgets are described in [Corsmeier et al., 2002; Junkermann et al., 2002; Moortgat et al., 2002; Platt et al., 2002; Winkler et al., 2002]

[9] The emphasis of PHOEBE was on the understanding of the local balance of the free radicals. (OH, HO<sub>2</sub> and RO<sub>2</sub> and NO<sub>3</sub>). For this purpose, measurements of the free radicals were performed at a selected site, Pabstthum, together with a large suite of comparatively stable chemical compounds, e.g., odd nitrogen compounds (NO, NO<sub>2</sub>, NO<sub>y</sub>, nonsoluble NO<sub>y</sub>, PAN), hydrocarbons and oxygenated

organic compounds (VOC), peroxides, ozone, CO, photolysis frequencies and meteorological parameters.

- [10] Specific questions addressed by PHOEBE were:
- 1. How do the concentrations of free radicals depend on the primary production, i.e.,  $Jo^1D$ , and on the concentrations of  $NO_x$  and VOC?
- 2. What is the influence of other sources (e.g., HONO photolysis and ozonolysis) on the radical concentrations?
- 3. How well do state of the art photochemical models reproduce the measured radical concentrations?
- 4. Is the photostationary state (PSS) approach a suitable tool to determine the local ozone production rate PO<sub>3</sub>?
- 5. What are the main sources of free radicals at night and how large is the influence of NO<sub>3</sub> radicals on the oxidation capacity of the atmosphere?
- [11] In this paper we describe the experimental setting of PHOEBE, give a summary of the many analytical techniques applied at Pabstthum and the experimental results, including instrument comparisons, and highlight the main scientific conclusions from the publications of this special section. The research groups that participated in PHOEBE are listed in Table 1.

## 2. Experimental

#### 2.1. The PHOEBE Site at Pabstthum

- [12] The PHOEBE site  $(12^{\circ}56'25''E, 52^{\circ}51'15''N, 50 \text{ m}$  above sea level) was established about 400 m east of the small village Pabstthum at the western border of a flat grassland of  $7.5 \times 4.5 \text{ km}^2$  extension (Figure 2). Selection criteria were the distance from Berlin in order to obtain a good representation of the plume development in conjunction with the other BERLIOZ sites (see Figure 1), as well as the absence of local anthropogenic sources, reasonably flat terrain with unrestricted flow from the direction of Berlin, and logistical requirements such as electrical power and road access for supplying liquid nitrogen and gases.
- [13] The area around Pabstthum, which itself consists of only 5 residences, is extremely sparsely populated. Local emissions from traffic, industry and residences in the vicinity of Pabstthum are negligible, except for the motorway A24 in the west about 10 km away. The nearest villages Wall and Radensleben located about 5 and 7 km to the SE and NW, respectively, have less than 500 inhabitants. The closest city is Neuruppin, 12 km in the NW, with 38,000 inhabitants. Berlin (3.4 million inhabitants) is located in southeasterly direction (140°) at a distance of about 50 km (city center).
- [14] A mixed forest dominated by Scots pine (*Pinus sylvestris*) extends from the station in westerly and northerly direction. About 50 m in westerly direction of the station is a line of Holm oaks (*Quercus ilex*) along the trail to the site. The grass land is used for cattle farming, except for an area of about 100 m in easterly direction, which was kept clear during the campaign.

#### 2.2. Instrumentation

[15] The instrumentation deployed at Pabstthum is summarized in Table 2 together with information on the time resolution of the measurements and the responsible institutions (cf. Table 1). More detailed information is found in the accompanying papers. The experimental setting of the

**Table 1.** Institutions Involved in PHOEBE

Acronym	Institution			
FZJ	Research Center Jülich, Institut für Chemie und Dynamik der Geosphäre			
IUP	University of Heidelberg, Institut für Umweltphysik			
IVD	University of Stuttgart, Institut für Dampfkesselwesen			
MPI-C	Max-Planck Institute for Chemistry, Mainz			
TUD	Technical University of Darmstadt, Institut für Chemie			

PHOEBE site is shown in Figures 3 and 4. In order to keep the influence of local surface emissions and deposition at a minimum, the instruments were placed as close together as possible at a height of approximately 10 m.

- [16] The instruments for odd nitrogen compounds, O<sub>3</sub>, CO, PAN, HCHO and speciated hydrocarbons were housed inside an air conditioned mobile laboratory. The inlets were mounted 10–11 m above ground on a pneumatic mast, which also carried a photometer for the measurement of J<sub>NO2</sub>. The gold converter for NO<sub>y</sub> was mounted directly at the inlet. Details are given by *Konrad et al.* [2003] and *Volz-Thomas et al.* [2003]. Air temperature, wind direction and wind speed were also measured at 11 m height on the same mast.
- [17] The cryogenic sampler of the MIESR (Matrix Isolation ESR Spectroscopy) was also operated on a pneumatic mast, 11 m above ground, about 10 m NE of the mobile laboratory. The samples were collected over 30 min intervals and analyzed after the campaign at the laboratory in Jülich [Mihelcic et al., 2003].
- [18] The LIF (Laser-Induced Resonance Fluorescence) instrument for the measurement of OH and HO<sub>2</sub> radicals was mounted inside a laboratory container which was placed on a 5 m high scaffolding platform. The inlet of the LIF instrument was 10 m above ground. Measurements of photolysis frequencies were made on the LIF container using a scanning spectral radiometer and two filter radiometers (JNO<sub>2</sub> and JO<sup>1</sup>D). Another container on the platform housed the sampling devices for the measurement of peroxides, carbonyl compounds and carboxylic acids [Grossmann et al., 2003] and a chemical amplifier for the measurement of peroxy radicals, i.e., the sum of HO<sub>2</sub> and RO<sub>2</sub> [Volz-Thomas et al., 2003].
- [19] A DOAS (Differential Optical Absorption Spectroscopy) system for the measurement of NO<sub>2</sub>, NO<sub>3</sub>, O<sub>3</sub>, HCHO and SO<sub>2</sub> was also mounted on the platform. It had a folded light path of a total length of more than 2 km (Multireflection Cell with 15 m base length, 144 reflections) [Alicke et al., 2003]. A second DOAS system (DOAS2) for the measurement of NO<sub>3</sub>, NO<sub>2</sub>, HONO, HCHO, SO<sub>2</sub>, O<sub>3</sub>, and aromatic VOC pointed in easterly direction from a height of 1.5 m at the station to a retroreflector mounted 36 m above the ground at a distance of 6.3 km [Geyer et al., 1999, 2003].
- [20] Vertical soundings of  $O_3$ ,  $NO_x$ , and meteorological parameters were conducted with a tethered balloon up to an altitude of 900 m. A second tethered balloon carried four automatic sampling units for hydrocarbons [Glaser et al., 2003].
- [21] The site was in operation from 13 July to 8 August. Most of the continuous in situ measurements, including

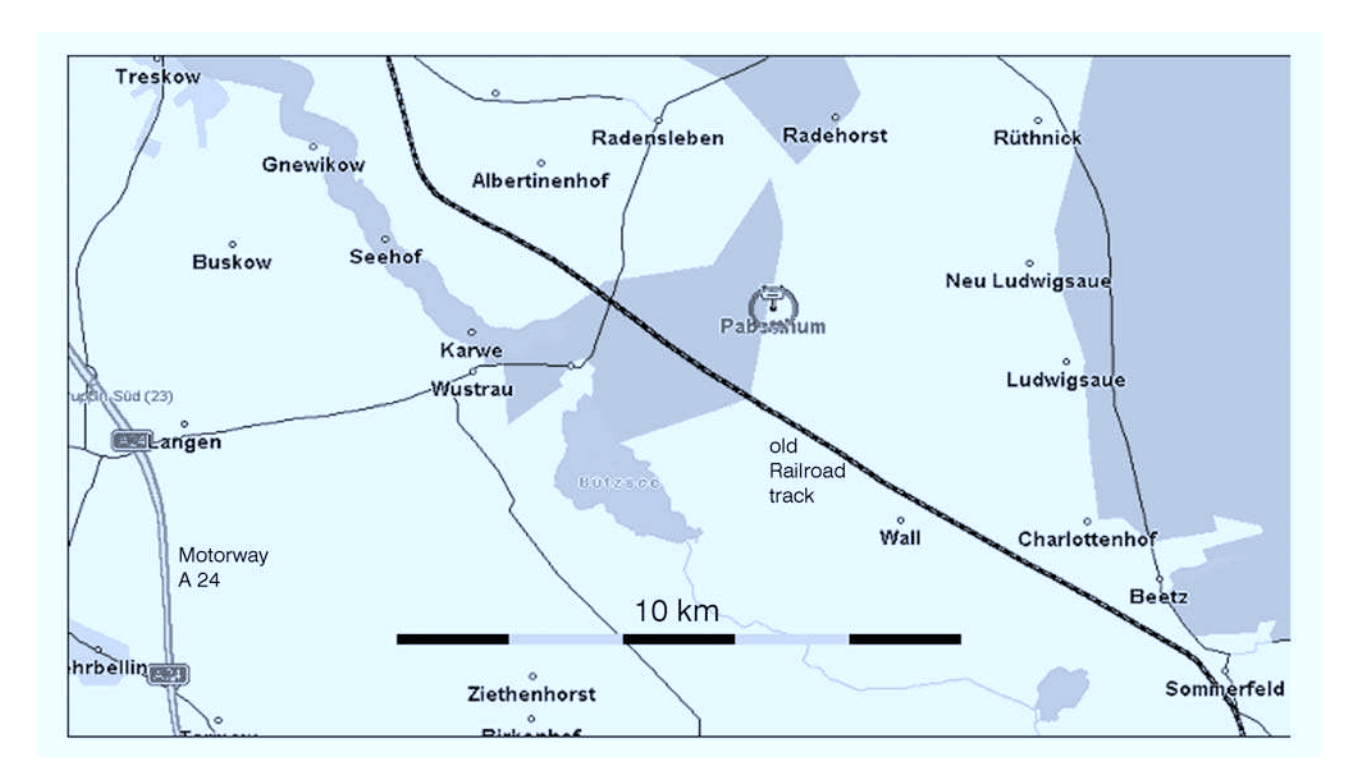


**Figure 2.** Surroundings of the PHOEBE observatory site Pabstthum (green: forested areas, blue: water bodies). See color version of this figure at back of this issue.

DOAS, LIF and the GCs, were conducted over the entire period and were interrupted only for calibration and maintenance, or during rain fall. The vertical soundings and some other experiments (i.e., MIESR, peroxides, carbonyl compounds and carboxylic acids), however, were limited in the number of samples. These measurements were concentrated on the intensive observational periods (IOPs) which took place on 20 and 21 July and 4 and 5 August upon announcement by the BERLIOZ steering group on the basis of weather forecasts. Thus, the full set of chemical measurements was available only during these time periods, on which the interpretation of the radical chemistry and the modeling work presented in this special section is concentrated.

#### 3. Meteorological Situation

[22] The meteorological situation during BERLIOZ was dominated by a westerly monsoon regime, which lasted unusually long. Winds between  $180^\circ$  and  $360^\circ$  prevailed more than 80% of the time (Figures 5 and 6), while southeasterly winds from the direction of the greater Berlin area  $(120^\circ-160^\circ)$  occurred only at about 3% of the time. This was not expected from the long term wind rose of Berlin exhibiting a secondary maximum at southeasterly directions with a probability of about 9% during July (E. Reimer, personal communication).

[23] Because of this situation, the PHOEBE site was under the influence of marine air for most of the time. The nearest larger cities in the west sector are Magdeburg (110 km, SW), Hamburg, (150 km, WNW), and Halle/Leipzig (170 km, SSW). The Ruhr Valley and the Frankfurt/Mannheim area are more than 400 km in the west and SW, respectively. The city plume of Berlin with photosmog

conditions was only observed on a few occasions, i.e., on 20, 21, and 23 July. On the first 2 days of this period an IOP was called by the BERLIOZ steering group. During the second IOP (3–5 August), the wind direction was NW so that Pabstthum was not under the influence of the Berlin plume, which was then to be detected by the southeasterly BERLIOZ sites.

# 3.1. Synoptic Situation on 20 July 1998

[24] Behind a strong low pressure system moving from the North Sea to the northern part of Scandinavia, a weak high-pressure system developed over Poland during the night of 19 and 20 July. At the same time warm air originating in the subtropics moved north over SW Germany, thereby pushing a warm front towards NE. The edge of the warm front reached Berlin during the early afternoon of 20 July with little weather activity (Figure 7). The arrival of the warm air was accompanied by low level stratiform clouds, which dissolved shortly after 8 UTC without any precipitation. The advection of warm air and the enhanced irradiance under clear skies led to a pronounced increase in temperature relative to the previous days. The maximum temperature of slightly above 30°C was 6°C higher than during the previous days.

[25] The surface wind at Pabstthum (10 m above ground) was calm during the night, increased after sunrise, and turned to southeasterly directions between 0500 and 0530 UTC. During the day the wind direction remained at about 160° until 18 UTC allowing the advection of air from the southwestern part of the greater Berlin area.

[26] Local profiles of potential temperature at Pabstthum [Glaser et al., 2003] showed the vertical development of the mixing layer from <100 m in the early morning to above

Table 2. Instrumentation Deployed at Pabstthum

Parameter	Instrument	Time resolution	Institution <sup>a</sup>	Reference
	Odd Nitrogen Comp	nounds		
NO	Chemiluminescence (770 Alppt, EcoPhysics)	1 min	FZJ	Volz-Thomas et al. [2003]
NO <sub>x</sub>	CLD 770 Alppt + PLC 760 (EcoPhysics)	1 min	FZJ	Volz-Thomas et al. [2003]
NO <sub>2</sub>	Differential optical absorption spectroscopy	30 min	IUP	Alicke et al. [2003]
1102	(DOAS 1 and 2)	30 mm	101	лиске ei ui. [2003]
NO <sub>2</sub> <sup>b</sup>	Matrix isolation and ESR spectroscopy (MIESR)	30 min	FZJ	Mihelcic et al. [2003]
$NO_v$	CLD 770 ALppt + Au-converter	1 min	FZJ	Volz-Thomas et al. [2003]
NO <sub>v</sub> -HNO <sub>3</sub>	CLD 770 ALppt + Au-converter + Denuder	1 min	FZJ	Volz-Thomas et al. [2003]
$HNO_2$	DOAS 1	30 min	IUP	Alicke et al. [2003]
PAN	GC-ECD (Meteorologieconsult)	6 min	FZJ	Volz-Thomas et al. [2003]
	O.4			
0	Other DOAS	20 min	IIID	41 also at al [2002]
$O_3$		30 min	IUP	Alicke et al. [2003]
$O_3$	UV Absorption (TE-49)	1 min	FZJ	Volz-Thomas et al. [2003]
H <sub>2</sub> O <sub>2</sub> , ROOH	Enzyme catalyzed fluorescence	23 min	MPI	Grossmann et al. [2003]
CO	IR Absorption (TE-48)	1 min	FZJ	Volz-Thomas et al. [2003]
CN	Condensation Nuclei Counter (TSI)	1 min	FZJ	Volz-Thomas et al. [2003]
$SO_2$	DOAS	30 min	IUP	Alicke et al. [2003]
	Organic Compou	ınds		
NMHC: C <sub>5</sub> -C <sub>10</sub>	In situ GC (Airmotec HC1010)	20 min	FZJ	Konrad et al. [2003]
NMHC: $C_2 - C_{10}$	In situ GC (HPGC/Cryogenic sampling)	85 min	FZJ	Konrad et al. [2003]
H <sub>2</sub> CO	Fluorescence (AeroLaser, AL4001)	1 min	FZJ	Volz-Thomas et al. [2003]
H <sub>2</sub> CO	DOAS	30 min	IUP	Alicke et al. [2003]
Carbonyl comp.b	Derivatization, GC/ECD	1 h	TUD	Grossmann et al. [2003]
Carboxylic acids <sup>b</sup>	Capillary Electrophoresis-LIF	1 h	TUD	Grossmann et al. [2003]
Aromatics, Phenols	DOAS	30 min	IUP	Alicke et al. [2003]
	Free Radicals	,		
ОН	LIF	90 s	FZJ	Holland et al. [2003]
HO <sub>2</sub>	LIF	90 s	FZJ	Holland et al. [2003]
HO <sub>2</sub> <sup>b</sup>	MIESR	30 min	FZJ	Mihelcic et al. [2003]
RO <sub>2</sub> <sup>b</sup>	MIESR	30 min	FZJ	Mihelcic et al. [2003]
$RO_x (HO_2 + RO_2)$	Chemical amplifier (CA)	72 s	MPI-C	Volz-Thomas et al. [2003]
$NO_3$	DOAS	30 min	IUP	Geyer et al. [1999, 2003]
NO <sub>3</sub> <sup>b</sup>	MIESR	30 min	FZJ	Mihelcic et al. [2003]
3		2.7		
T II D ' 1 .	Meteorology and Ra		DZI	II 1 TI
T, rH, P, wind vector	Psychrometer, wind vane, cup anemometer (Thiess)	1 min	FZJ	Volz-Thomas et al. [2003]
Global radiation	Pyranometer (Kipp&Zonen)	1 min	FZJ	Volz-Thomas et al. [2003]
JO <sup>1</sup> D, JNO <sub>2</sub>	$2\pi$ sr filter radiometers	10 s	FZJ	Holland et al. [2003]
JNO <sub>3</sub>	$2\pi$ sr filter radiometer	10 s	IUP	Gever et al. [1999, 2003]
Ji,j (actinic flux)	$2\pi$ sr spectral radiometer (Bentham)	90 s	FZJ	Holland et al. [2003]
	Vertical Profiles (Tethere	ed Ralloon)		
$O_3$	Chemiluminescence (GFAS, OS-B-2)	га Банооп) 10 s	IVD	Glaser et al. [2003]
NO <sub>2</sub> and NO <sub>x</sub>	Luminol chemiluminescence (Scintrex, LMA-4)	10 s 10 s	IVD	Glaser et al. [2003]
NMHC <sup>b</sup>	Adsorption tubes, GC/FID	3 h	IVD	Glaser et al. [2003]
T, rH, P, wind vector	Meteorological Sonde (Atmos. Instr. Res. Inc.)	10 s	IVD	Glaser et al. [2003] Glaser et al. [2003]
<sup>a</sup> See Table 1	Treesorological bonde (Aunos, msu, res. me.)	10 3	111	5145C1 C1 41. [2003]

<sup>&</sup>lt;sup>a</sup>See Table 1.

900 m (the ceiling altitude of the balloon) at 11 UTC lasting until late afternoon. The analysis by *Corsmeier et al.* [2002] for the entire BERLIOZ area and including the aircraft measurements confirmed the well defined planetary boundary layer (PBL) with southeasterly wind directions and a sharp transition to southwesterly winds in the free troposphere. According to the aircraft data, the PBL rose between 6 and 12 UTC to approx. 900 m and developed further to 1.4 km. In the late afternoon, the vertical extent of the southerly wind regime decreased again to approx. 1 km around 18 UTC. In the evening, the westerly wind regime proceeded downward by the combined action of the diurnal change in the heat balance and the shear-induced turbulence at the top of the PBL. Due to the latter, transport conditions

were not as well defined as intended for the BERLIOZ experiment.

#### 3.2. Synoptic Situation on 21 July 1998

[27] Another low pressure system moved slowly NE ward from Scotland on 20 July (Figure 7). Advection of hot air ahead of the system lead to temperatures well above 30°C in Berlin on 21 July. Starting sunny in the morning clouds developed during the day while a frontal system that had originated in the morning west of Berlin moved eastward creating some precipitation in isolated showers and thunderstorms. Ahead of the convergence the wind direction turned towards SE. During the day the winds moved on to westerly directions just behind the frontal system bringing in slightly

<sup>&</sup>lt;sup>b</sup>Off-line samples collected only during IOPs.

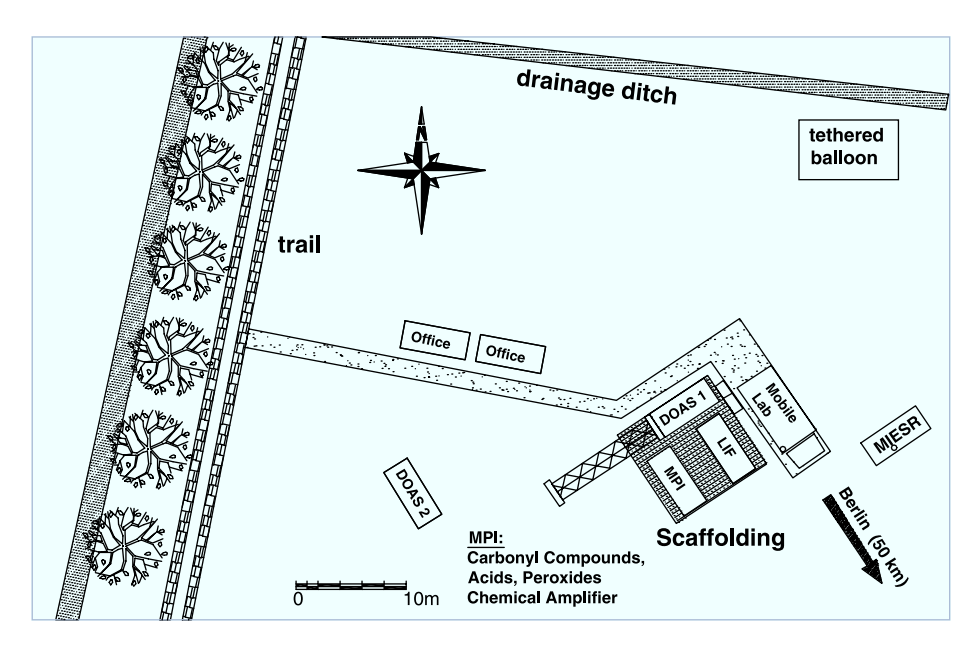
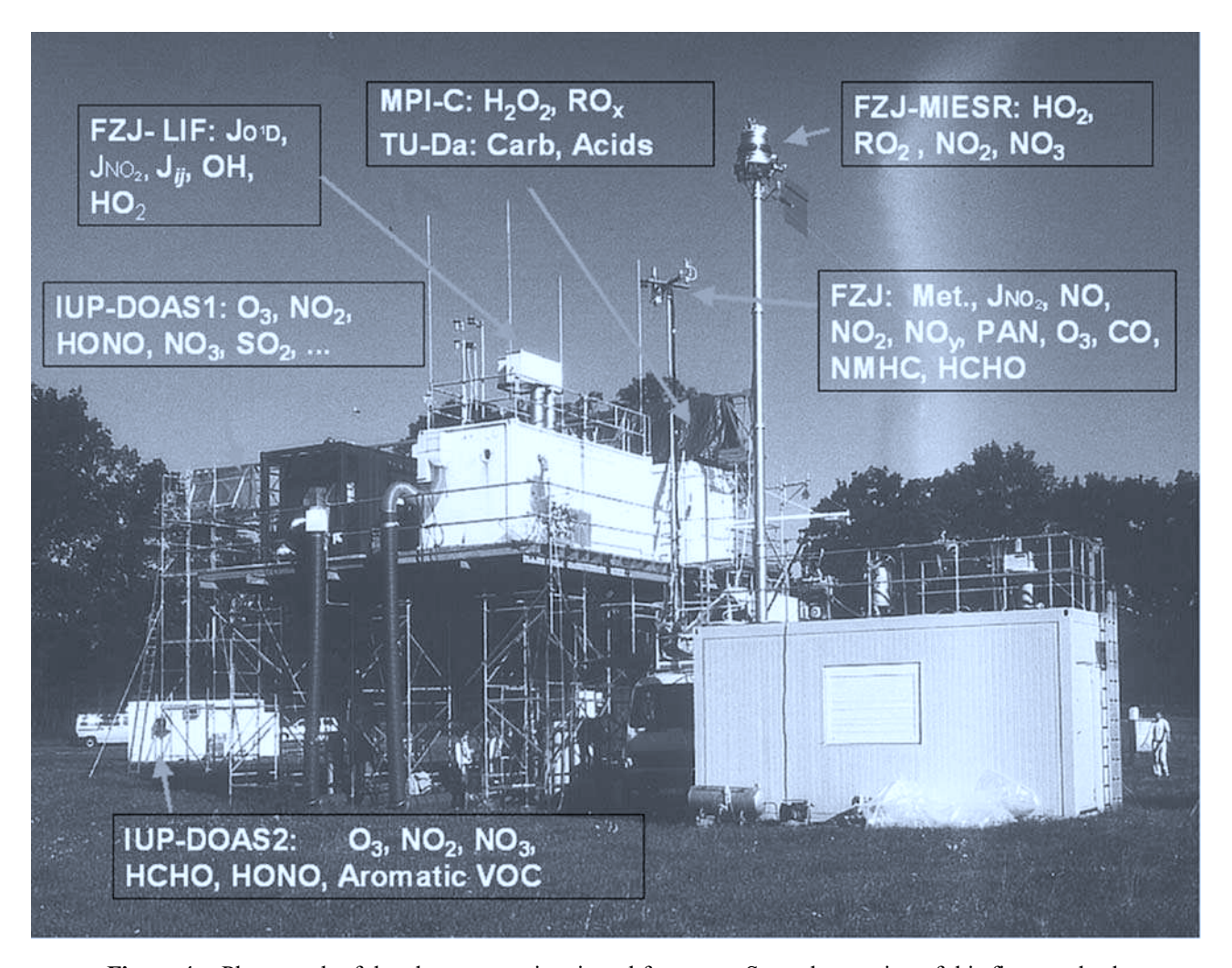
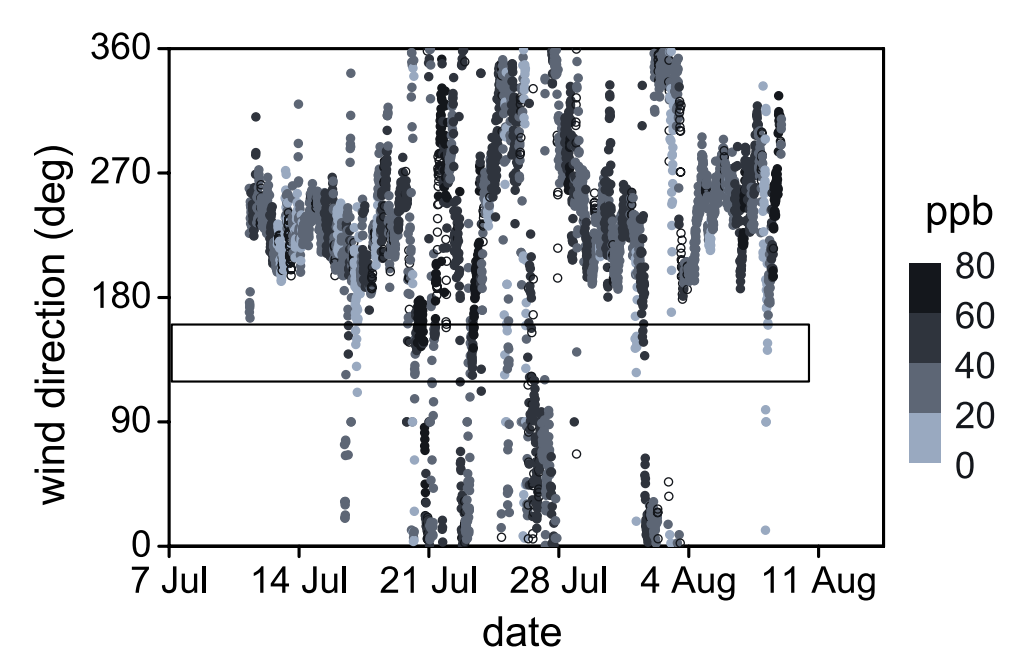


Figure 3. Schematic arrangement of the individual measuring systems at the observatory site.



**Figure 4.** Photograph of the observatory site viewed from east. See color version of this figure at back of this issue.



**Figure 5.** Time series of the wind direction at Pabstthum during the BERLIOZ campaign (10 min averages). The box indicates the sector for winds coming from the greater Berlin area. Colors denote the  $O_x$  mixing ratio (black circles: missing  $O_x$  values). See color version of this figure at back of this issue.

dryer and colder air masses than before. The wind speed was generally lower than on 20 July and decreased further except for some isolated gusts in the greater Berlin area.

[28] At Pabstthum, wind from SE was observed shortly after 6 UTC for about 2 hours. After 8 UTC, the wind turned to SW and west throughout the whole boundary layer. Wind speed at the surface was low with 2–4 m/s. In contrast wind speeds at 200 m above ground were much higher reaching

more than 10 m/s. A mixing layer depth of only 200 m was observed in the morning increasing to about 500 m at 12 UTC [Glaser et al., 2003]. Cloudiness increased after 11 UTC diminishing gradually the insolation.

# 3.3. Synoptic Situation on 3 and 4 August

[29] The general meteorological situation was characterized by a pronounced trough over western Europe at 500

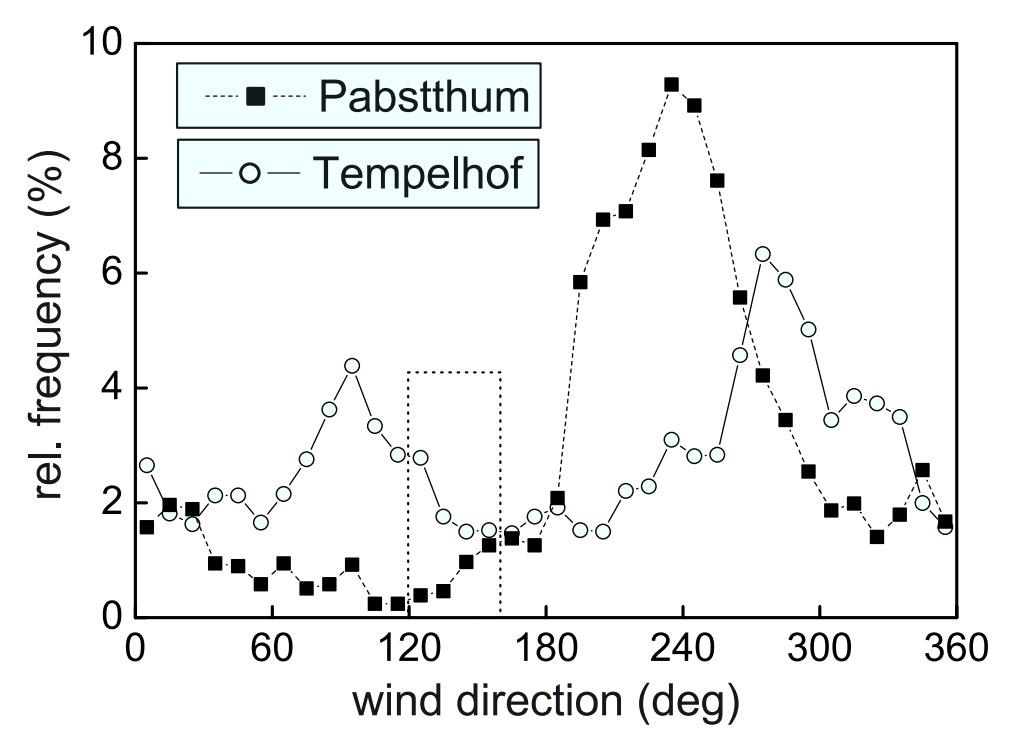


**Figure 6.** Frequency distribution of the wind direction at Pabstthum during BERLIOZ (squares) compared to the long-term distribution for summer at Berlin-Tempelhof (open circles).

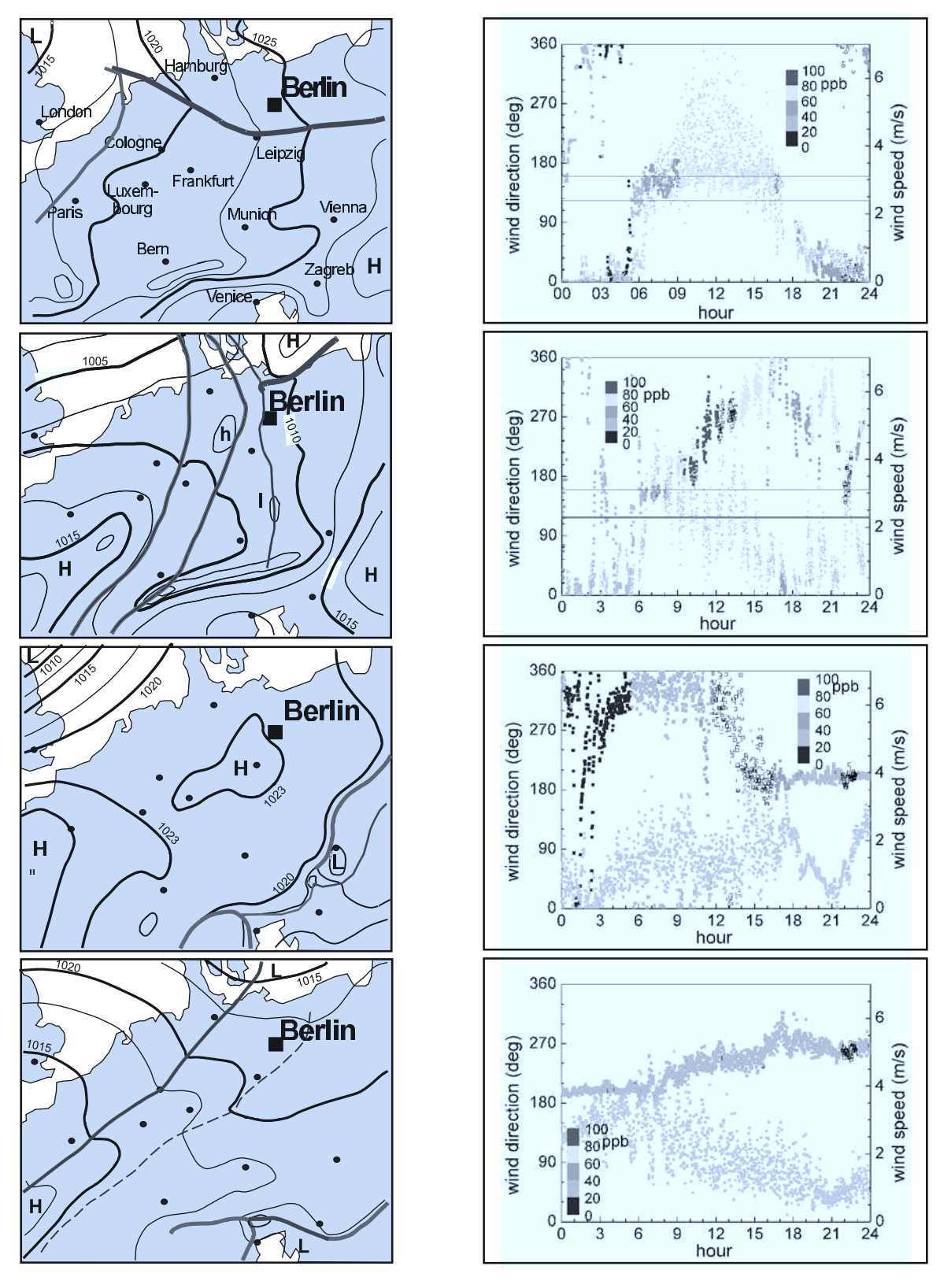


**Figure 7.** Meteorological surface charts for 12 UTC (left) and surface wind (at 10 m above ground) at Pabstthum (right) for 20 July (top), 21 July, 3 August, and 4 August (bottom). The color code in the wind direction denotes the  $O_x$  mixing ratio (black circles: missing  $O_x$  values; gray dots: wind speed). See color version of this figure at back of this issue.

hPa moving slowly eastward (Figure 7). An intense cutoff low developed on the 3 August and moved into the Gulf of Genoa. Westerlies with high wind speeds in the free troposphere prevailed over Central Europe. A high-pressure ridge that stretched from the Azores to northern Scandinavia on 3 August, moved southward and covered most of the middle and northern parts of Europe, before it was replaced by frontal systems moving from the North Sea to Poland on 4 August.

[30] On the southern edge of the high pressure, winds from northerly directions were observed at 2 and 3 August over the BERLIOZ region, turning south after noon on 3 August behind a weak front transporting warm air quickly from mid-Atlantic ocean to the BERLIOZ region. The balloon profiles [Glaser et al., 2003] showed that surface winds prevailed throughout the boundary layer. After the passage of the cold front between 6 and 9 UT on 4 August, the wind direction changed to SW and to west in the afternoon behind an occlusion. Moderately warm air originating at subpolar regions was advected with the frontal systems.

[31] The surface wind speed on average did not exceed 2 m/s on 3 August but was highly variable with gusts up to 4 m/s. During to the warm front passage the speed decreased but increased before midnight of the 3rd ahead of the first cold front reaching about 3.5 and 4.5 m/s during gusts around 9 UT on 4 August. After the passage of the first and the second cold front speed decreased continuously. During night between 4 and 5 August, when measurements of NO<sub>3</sub> radicals were made, surface winds were calm between 0.5 and 1 m/s. Under decreasing cloud cover, a stable surface layer developed during the night. In the early morning, a shallow fog layer developed at Pabstthum.

# 4. Main Results From the Accompanying Papers4.1. Data Quality and Instrument Comparisons

[32] Quality assurance was an important aspect in BER-LIOZ. It served the purpose to assess the accuracy of each measurement and to ensure the consistency of calibrations of different instruments that measured the same quantity during the campaign. Intercomparisons were performed at different times. Photolysis frequency instruments, which participated in BERLIOZ, were compared in advance against reference techniques during the field experiment JCOM97 in summer 1997 at Jülich [Kraus et al., 1998; Kraus et al., 2000]. Most other in situ instruments (VOC, NO<sub>x</sub>, CO, O<sub>3</sub>, PAN, HCHO) were brought together 1 week before the campaign at the airfield Schönhagen, where the measurements of all participants were formally calibrated against certified standards and compared to reference instruments in ambient air [Kanter et al., 2002; Volz-Thomas et al., 2002]. Even more intensive, albeit informal, comparisons were made at Pabstthum where most of the free radicals (HO<sub>2</sub>, HO<sub>2</sub> + RO<sub>2</sub>, NO<sub>3</sub>) and longer-lived compounds (O<sub>3</sub>, NO<sub>x</sub>, HCHO) were measured with different techniques [Geyer et al., 1999; Platt et al., 2002; Volz-Thomas et al., 2003].

# 4.1.1. Radicals

[33] Hydroxyl was measured by only one technique, laser-induced fluorescence (LIF), at Pabstthum [Holland et al., 2003]. The instrument and its calibration has been

compared previously against an absolute laser absorption spectrometer (DOAS) in a different campaign (POPCORN) where good agreement had been found [Hofzumahaus et al., 1998]. The same calibration method, the 185 nm photolysis of water vapor in synthetic air yielding OH and HO<sub>2</sub>, was applied during BERLIOZ where the estimated  $2\sigma$ -calibration error was 20% for both radicals.

[34] At Pabstthum the LIF instrument was also used for the measurement of  $HO_2$  concentrations, which were calibrated with the same radical source as for OH. On 2 days (20 and 21 July 2001)  $HO_2$  was measured additionally by MIESR, an absolute technique with an estimated accuracy of 5% [Mihelcic et al., 2003]. The correlation of the temporally overlapping measurements was linear ( $R^2 = 0.88$ ) and showed a good agreement with a slope of 1.03, well within the combined uncertainty of both instruments [Platt et al., 2002].

[35] Measurements of speciated peroxy radicals (HO<sub>2</sub>, CH<sub>3</sub>COO<sub>2</sub>, and the sum of all other organic peroxy radicals RO<sub>2</sub>) were performed by MIESR, each with an accuracy of 5% [*Mihelcic et al.*, 2003]. The sum of all peroxy radicals (HO<sub>2</sub> + RO<sub>2</sub>) was also recorded by a chemical amplifier with a calibration uncertainty of 20% [*Volz-Thomas et al.*, 2003]. The comparison of both techniques showed good agreement, the chemical amplifier data being about 7% lower than the MIESR measurements, again well within the estimated calibration errors.

[36] Simultaneous  $NO_3$  measurements were achieved in the night of 4 and 5 August by MIESR and the DOAS2, which was operated with a single-folded light path over a distance of 6.3 km. Despite of relatively low concentrations, the comparison of the DOAS and MIESR data sets showed a tight linear correlation ( $R^2 = 0.98$ ). The systematic deviation of 17% is within the combined systematic errors of both measurement techniques [Geyer et al., 1999], although the influence of spatial inhomogeneity cannot be excluded completely.

#### 4.1.2. Photolysis Frequencies

[37] A scanning spectroradiometer was deployed at Pabstthum to measure absolute spectra of the solar actinic flux from which photolysis frequencies of different species  $(O_3, NO_2, HCHO, H_2O_2, HONO, CH_3OOH, CH_3CHO)$ were derived [Holland et al., 2003]. The actinic flux calibration was performed using certified UV lamps traceable to national standards (PTB, Germany). The spectra were evaluated using the quantum yield of Matsumi et al. [2002]. In a previous campaign JO<sup>1</sup>D determined by the spectroradiometer had been compared against a chemical JO<sup>1</sup>D actinometer. Agreement was found within 14% which could be explained by the uncertainties of both measurement techniques [Müller et al., 1995]. The spectroradiometer and two independent chemical JNO<sub>2</sub> actinometers were compared during JCOM97. All three instruments agreed within 7% over a large range of solar zenith angles  $(<80^{\circ})$  [Kraus et al., 1998, 2000; Junkermann et al., 2002].

[38] A number of commercial fixed-bandwidth filter radiometers (Meteorologieconsult, Glashütten) were used to measure JNO<sub>2</sub> at most BERLIOZ sites. During JCOM97, all filter radiometers (N = 11) showed consistent calibrations within 4% ( $2\sigma$ ) and agreed on average within 4% with two different chemical actinometers [*Kraus et al.*, 1998]. During BERLIOZ, two of the filter radiometers and the

spectroradiometer measured simultaneously at Pabstthum. The agreement was on average within 2.5% for solar zenith angles less than 70° [Holland et al., 2003]. No independent comparison was possible for JO¹D, since the additional filter radiometer deployed for JO¹D at Pabstthum was calibrated against the spectroradiometer measurements.

# 4.1.3. $NO_x$ , $O_3$ , CO, and PAN

- [39] As outlined by *Kanter et al.* [2002], the O<sub>3</sub> monitor deployed at Pabstthum agreed within 5% with a reference instrument that was calibrated against the NIST traceable primary standard of the Eidgenössische Materialprüfungsund Forschungsanstalt (EMPA, Dübendorf, CH). For quality assurance of CO, two canister samples were collected at Pabstthum and measured against certified standards traceable to NOAA CMDL, Boulder (3–8% disagreement with the reference). The dynamic PAN calibration systems [*Pätz et al.*, 2002] used by the different investigators agreed within 10% [*Kanter et al.*, 2002].
- [40] For NO<sub>2</sub>, NO<sub>y</sub>, and PAN, the instruments described in this paper served as the reference in BERLIOZ. The NO standard used at Pabstthum for calibration of all four CLDs agreed within 1% with the BERLIOZ reference standard (NIST traceable via EMPA). The data quality of the NO<sub>2</sub> measurements was investigated by comparison of the simultaneous measurements made at Pabstthum by CLD/PLC, DOAS, MIESR, and with the balloon borne LMA4 instrument (cf. Table 2). Although the comparison was not organized in a strictly blind fashion, the different instruments had been calibrated independently and the data were not harmonized before the comparison. On average, the deviation between the four techniques was less than 5% with slightly higher values determined by the spectroscopic methods [Volz-Thomas et al., 2003].
- [41] The agreement for  $NO_x$  (NO and  $NO_2$ ), between the balloon borne LMA4 instrument employing conversion of NO to  $NO_2$  on  $Cr_2O_6$  and the ground based CLD/PLC instrument was similarly good as for the  $NO_2$  measurements. A direct comparison of the NO concentrations was not possible as the LMA4 on the tethered balloon measured  $NO_x$  and  $NO_2$  sequentially and thus at different heights [Volz-Thomas et al., 2003].

#### 4.1.4. VOC

- [42] The characterization and harmonization of the different in situ GC systems (10 different laboratories with almost 20 instruments) deployed in BERLIOZ was a major task of the quality assurance activities. Because of the many new systems deployed and the involvement of groups with varying experience in field measurements, the activities involved several comparisons of standard mixtures before a final assessment of instrument performance was made by a comparison in ambient air at Schönhagen [Volz-Thomas et al., 2002].
- [43] Non methane hydrocarbons (NMHC) were determined at Pabstthum by in situ gas chromatography with two different systems, namely an Airmotec HC1010 and a custom made system built around a HP5890 (referred to as HP-GC). The HC1010 is appropriate for measuring  $C_5-C_{10}$  HC with a time resolution of 20 min, whereas the HP-GC is suitable for  $C_2-C_{10}$  HC with an 80–90 min measuring cycle. The HP-GC had been elected as the reference instrument for the overall quality assurance in BERLIOZ [*Volz-Thomas et al.*, 2002]. A comparison of the two GCs and

tests performed with the inlet system are described by Konrad et al. [2003] and Konrad and Volz-Thomas [2000].

[44] The DOAS system was also set up to measure several aromatic hydrocarbons, as well as phenols and cresols. While some of these compounds were indeed found at significant levels at Eichstädt, the concentrations at Pabstthum remained always below the detection limit of the DOAS system so that a comparison with the GCs was not possible.

### 4.1.5. Formaldehyde

[45] Several commercial monitors (AeroLaser) that utilize fluorescence for detection of HCHO following the Hantzsch reaction were deployed at the different BERLIOZ sites. Calibration of the monitors was based on a common liquid standard provided by the University of Wuppertal. The comparison at Schönhagen [Kanter et al., 2002] was formally satisfying, although somewhat hampered by very low concentrations. At Pabstthum, HCHO was also measured by DOAS [Alicke et al., 2003]. The mixing ratios measured by DOAS (max. 7.7 ppb) were systematically larger by a factor 1.3 on average and by a factor 1.7 during high photochemical activity [Grossmann et al., 2003]. An even larger discrepancy between Hantzsch and DOAS was observed at the BERLIOZ sites Eichstädt and Blossin (see Figure 1). Grossmann et al. [2003] discuss the possible reasons for the discrepancy in the light of results from other comparisons and conclude that none of the two measurements at Pabstthum can be proven wrong on the basis of the existing information and that the unresolved discrepancy of about a factor of two must be included in the uncertainty of [HCHO] for model simulations of the radical budgets (see below). Further comparison of the different methods for the measurement of HCHO under atmospheric conditions certainly remains an important task.

#### 4.2. Observational Results

#### 4.2.1. OH Radicals

- [46] OH radical concentrations were measured by LIF for the time period from 20 July to 6 August with a typical time resolution of 90 s [Holland et al., 2003]. The variability of OH was mainly controlled by changes in the solar UV responsible for the photochemical formation of OH [Holland et al., 2003]. Daily maxima of OH were usually observed at midday and showed values in the range of  $(4-8) \times 10^6$  cm<sup>-3</sup>. The shape of the diurnal OH profiles followed closely the variations of JO<sup>1</sup>D with a linear correlation coefficient of R  $\sim$  0.9. During the early morning and late evening hours, however, OH concentrations as high as  $1.5 \times 10^6$  cm<sup>-3</sup> were measured even when JO<sup>1</sup>D was essentially zero. This behavior can be attributed to the radical production by photolysis of HONO and HCHO. These precursors were found to be efficient photochemical sources of OH under polluted conditions like in the morning of 20 and 21 July [Alicke et al., 2003]. At sunset the observed OH may be explained as a result of reactions of O<sub>3</sub> and NO<sub>3</sub> radicals with alkenes [Geyer et al., 1999, 2003].
- [47]  $NO_x$  was found to be another important parameter that controls OH. This is seen in the  $JO^1D$ -normalized OH data which exhibit a nonlinear  $NO_x$  dependence with a maximum around 3 ppb  $NO_x$  [Holland et al., 2003]. Towards lower  $NO_x$  levels the OH concentrations decline due to the decreasing conversion of  $HO_2$  into OH by

reaction with NO (R4), whereas towards higher NO<sub>x</sub> levels the OH concentrations decrease due to increasing depletion of OH by reaction with NO<sub>2</sub>(R13). In comparison to the field campaign POPCORN, which took place in a clean rural environment [*Plass-Dülmer et al.*, 1998], the OH data from BERLIOZ are about a factor of 2 lower for the same values of JO<sup>1</sup>D and NO<sub>x</sub> [*Holland et al.*, 2003].

[48] At night, OH concentrations were usually below the detection limit of the LIF when short integration times (90 s) were applied. Averaging the data over time intervals of 20 min yielded significant OH concentrations of  $(1.9 \pm 0.8) \times 10^5$  cm<sup>-3</sup> in the night of 20 and 21 July, which could be explained by the nocturnal production of OH from the reactions of biogenic monoterpenes with O<sub>3</sub> and NO<sub>3</sub> radicals [Geyer et al., 2003]. Averaging all nocturnal OH data measured at Pabstthum between 2100 and 0300 UT, yielded an experimental upper limit of  $5 \times 10^4$  cm<sup>-3</sup> for nocturnal OH [Holland et al., 2003].

#### 4.2.2. HO<sub>2</sub> Radicals

- [49] HO<sub>2</sub> radicals were measured by the LIF technique following the conversion of HO<sub>2</sub> into OH in the measurement system by added NO [Holland et al., 2003]. Two independent detection channels were run in parallel to measure HO<sub>2</sub> and OH simultaneously from 20 July to 6 August. Additional HO<sub>2</sub> concentrations were measured by MIESR on 20 and 21 July during daytime [Mihelcic et al., 2003] and in the night of 4 and 5 August 1998 [Geyer et al., 2003].
- [50] The  $\rm HO_2$  concentration showed daytime maxima due to photochemical formation [Holland et al., 2003]. The highest value (8  $\times$  10<sup>8</sup> cm<sup>-3</sup>, i.e., 32 ppt) was observed at noon on 21 July, a day which was characterized by exceptionally high VOC mixing ratios [cf. Konrad et al., 2003]. On other days the daily maxima were in the range of (2–4)  $\times$  10<sup>8</sup> cm<sup>-3</sup> (8–16 ppt).  $\rm HO_2$  exhibited a much less pronounced dependence on the solar UV then OH.  $\rm HO_2$  was strongly influenced by NO, which efficiently converts the peroxy radicals into OH by reaction (R4). In the morning hours (0400–1000 UT) when NO usually exhibited a morning peak, the  $\rm HO_2$  concentration was typically close to or below the detection limit.
- [51] After sunset HO<sub>2</sub> usually remained at significant levels above the detection limit  $(1 \times 10^7 \text{ cm}^{-3})$  and had an average nighttime value of  $3 \times 10^7 \text{ cm}^{-3}$  (~1 ppt). On some occasions HO<sub>2</sub> even increased after sunset as a result of HO<sub>2</sub> production by the reaction of biogenic VOCs with NO<sub>3</sub> and O<sub>3</sub> [Geyer et al., 2003]. The highest nocturnal HO<sub>2</sub> value  $(1 \times 10^8 \text{ cm}^{-3}, \text{ i.e., 4 ppt)}$  was observed in the night from 20 to 21 July when very high mixing ratios of organic species were encountered (e.g., up to ~0.5 ppb α-pinene). From midnight to sunrise the HO<sub>2</sub> concentrations usually decayed and reached values near the detection limit in the early morning as mentioned above.

#### 4.2.3. RO<sub>2</sub> Radicals

[52] Measurements of speciated peroxy radicals ( $\rm HO_2$ ,  $\rm CH_3COO_2$ ) and of the sum of all other organic peroxy radicals ( $\rm RO_2$ ) were performed by MIESR at daytime on 20 and 21 July and at nighttime between 4 and 5 August [*Mihelcic et al.*, 2003]. In addition continuous measurements of the total sum of all peroxy radicals ( $\rm HO_2 + RO_2$ ) were performed by a chemical amplifier from 12 July to 3 August [*Volz-Thomas et al.*, 2003]. In general the variations

of the diurnal profiles of RO<sub>2</sub> and HO<sub>2</sub> showed a great similarity. Like HO<sub>2</sub> the RO<sub>2</sub> radicals were often close to the detection limit in the morning due to elevated NO mixing ratios. The daily maxima of RO<sub>2</sub> occurred typically 1-2 hours after local noon and reached the highest value, about 20 ppt (i.e.,  $\sim$ 55 ppt of HO<sub>2</sub> + RO<sub>2</sub>), on 21 July 1998 [Mihelcic et al., 2003; Volz-Thomas et al., 2003]. The concentration of CH<sub>3</sub>COO<sub>2</sub> never exceeded the limit of detection (2 ppt) of the MIESR. The sum of other organic peroxy radicals measured by MIESR during daytime was about the same as the concentration of HO<sub>2</sub>. This result is consistent with ratios of (HO<sub>2</sub> + RO<sub>2</sub>)/HO<sub>2</sub> determined from the chemical amplifier and LIF technique. At noon of 20 and 21 July the ratio had a value around 2, but was higher  $(\sim 3)$  in the morning and evening hours [cf. Platt et al., 2002].

[53] At night the RO<sub>2</sub> radicals had much higher concentrations than HO<sub>2</sub>. For example the highest value of HO<sub>2</sub> + RO<sub>2</sub> was 22 ppt, whereas the maximum HO<sub>2</sub> value was 4 ppt [Geyer et al., 2003]. During many nights a significant increase of HO<sub>2</sub> + RO<sub>2</sub> was observed after sunset as a result of the reaction of NO<sub>3</sub> radicals with biogenic monoterpenes. In these cases the HO<sub>2</sub> + RO<sub>2</sub> concentration started from typically 3–4 ppt and reached a maximum of about 6 ppt between 2000 and 2200 UT. For the rest of the night RO<sub>2</sub> generally decreased together with HO<sub>2</sub> and reached a minimum at sunrise when NO started to increase [Geyer et al., 2003].

#### 4.2.4. NO<sub>3</sub> Radicals

- [54] Nitrate radicals were measured by the DOAS technique along a 12.6 km light path running at an average height of 18 m above the ground between the Pabstthum site and a reflector at 6.3 km distance [Geyer et al., 2003]. Since NO<sub>3</sub> is rapidly photolyzed during daytime, measurements were performed continuously from 17 July to 8 August between dusk and dawn only. In the night from 4 to 5 August NO<sub>3</sub> measurements were also performed by MIESR at the Pabstthum site and found to be in reasonable agreement with DOAS [Geyer et al., 1999].
- [55] The mixing ratios obtained by DOAS exceeded the detection limit of 2.4 ppt in 15 nights. Nighttime maxima were usually of the order of 10 ppt [Geyer et al., 2003]. In one night the NO<sub>3</sub> mixing ratio reached 70 ppt due to an exceptional high production rate of nitrate radicals by the reaction of NO<sub>2</sub> with O<sub>3</sub>. Similar time series of NO<sub>3</sub> were measured at the BERLIOZ sites Lindenberg, Blossin, and Eichstädt, where other DOAS instruments were operated. A correlation of the nighttime levels of NO<sub>3</sub> was observed among all four measurement sites [Platt et al., 2002].
- [56] At Pabstthum the average nighttime profile of  $NO_3$  started to rise above the detection limit around sunset and reached a maximum between 2000 and 2200 UT, followed by a continuous decay reaching levels below the detection limit at sunrise [Geyer et al., 2003]. This time profile was found to have a positive, linear correlation with the concentration of  $HO_2 + RO_2$  which also exhibited a nighttime maximum before midnight. For example, in the night of 4 and 5 August the correlation coefficient was  $R^2 = 0.83$ . The observed correlation can be described generally by a chemistry model showing that the nighttime  $HO_2$  and  $RO_2$  radicals were largely formed by the reaction of  $NO_3$  with biogenic VOCs at Pabstthum [Geyer et al., 2003].

# 4.2.5. VOC

[57] More than 60 hydrocarbons (NMHC) in the range of  $C_2-C_{10}$  were identified and quantified with the two GC systems deployed at Pabstthum [Konrad et al., 2003]. The data sets from both GC systems were combined to join the high time resolution of the HC1010 with the high precision and the larger number of measurable compounds on the HP-GC. This was achieved by interpolation between two data points of the HP-GC with the pattern given by the HC1010. For compounds that could not be reliably measured with the HC1010, patterns of compounds with similar reactivity were used.

[58] Air masses with the lowest photochemical age as estimated from the toluene/benzene ratio and the highest hydrocarbon mixing ratios were observed on 20 and 21 July when air was advected from the direction of Berlin. Alkanes were the most abundant hydrocarbons ( $\sim$ 60%) on a molecular basis, followed by alkenes and aromatics. The reactivity of the hydrocarbons towards OH, however, was dominated by the alkenes (>60%), with the biogenic hydrocarbons isoprene and  $\alpha$ -pinene constituting the major fraction even during the time when the site was under the influence of air from the greater Berlin area.

# 4.2.6. Oxygenated VOC

[59] Up to 30 different aldehydes and ketones ( $\geq C_2$ ) were identified and quantified at Pabstthum during the IOPs using a novel analytical technique (derivatization with PFBHA on cartridges, followed by GC-ECD analysis in the laboratory [Schlomski et al., 1997]). HCHO was measured continuously by both, DOAS and a commercial Hantzsch monitor (see above).

[60] Carboxylic acids (C<sub>1</sub>–C<sub>9</sub>) were sampled with a new optimized scrubber system. The samples were analyzed by sequential reaction with dicyclohexylcarbodiimide and 4-aminofluoresceine, followed by capillary zone electrophoresis (CEP) and detection by LIF [*Kibler et al.*, 1999]. These measurements were made during the IOPs only.

[61] Grossmann et al. [2003] discuss the diurnal variation of the oxygenated compounds and the correlation between primary and the secondary species that were observed at Pabstthum. The C<sub>2</sub>-C<sub>10</sub> aldehydes, which originate primarily from anthropogenic hydrocarbon degradation processes, showed maximum mixing ratios from 0.6 ppb (C<sub>2</sub>) to 0.1 ppb (C<sub>5</sub>). The C<sub>6</sub>, C<sub>9</sub> and C<sub>10</sub> alkanals exhibited strong fluctuations, thus giving evidence of biogenic emissions. The primary unsaturated carbonyl compounds (methylvinylketone and methacrolein) and the secondary oxidation products of isoprene (hydroxyacetone and glycolaldehyde) showed excellent correlation. Also, diurnal profiles of glyoxal, methylglyoxal, biacetyl, benzaldehyde, and pinon-aldehyde were obtained.

[62] Formic and acetic acid varied between 0.6 and 2.6 ppb. The mixing ratio of the other acids decreased from 0.1 to 0.2 ppb for  $C_3$  to a few ppt for the  $C_9$  monocarboxylic acids. The measurements highlight the importance of carbonyl compounds for accurately determining the total VOC reactivity. In some cases, important information on the chemical mechanism is derived from the observed correlation between precursors and oxidation products.

#### 4.2.7. PAN

[63] The PAN concentrations measured at Pabstthum were similar as on the other BERLIOZ sites, with maximum

mixing ratios around 1 ppb observed on the afternoon of 20 and 21 July. Because of the high temperatures on these days, PAN was an important source of peroxy radicals [Konrad et al., 2003] despite the low concentrations. On the other days with westerly winds, PAN usually remained around a few hundred ppt [Volz-Thomas et al., 2003].

#### 4.2.8. Peroxides

[64] The hydroperoxides show pronounced diurnal variations with peak mixing ratios in the early afternoon. The maximum mixing ratios were observed on 21 July (1.4 ppb  $\rm H_2O_2$ , 0.64 ppb methylhydroperoxide, and 0.22 ppb hydroxymethyl-hydroperoxide). The increase of  $\rm H_2O_2$  in the morning originated mainly from vertical transport from the residual layer and changes in advection. A secondary maximum sometimes observed in the late afternoon indicates the formation from ozonolysis of biogenic alkenes. The  $\rm H_2O_2/HNO_3$  ratio is used as indicator for distinguishing between  $\rm NO_x$  and VOC limitation of photochemical ozone production at Pabstthum [*Grossmann et al.*, 2003].

# 4.2.9. Odd Nitrogen Compounds and Photostationary State of $NO_x$

[65] As observed in several other campaigns, the measured NO/NO<sub>2</sub> ratio was found to be significantly larger than that calculated from either the box models (see below) or from the so-called photostationary state, i.e., by assuming quasi steady state between the NO<sub>2</sub> photolysis rate and the oxidation rate of NO provided by reactions with  $O_3$ ,  $HO_2$ , and RO<sub>2</sub>. The PSS approach was shown to severely overestimate the local ozone formation rate as determined from the measured NO and radical concentrations and the accepted rate coefficients [Mihelcic et al., 2003; Volz-Thomas et al., 2003]. Faster rate coefficients for the reaction of RO2 with NO, as discussed by Frost et al. [1998], are not considered a likely explanation, because the discrepancy exists also at high NO concentrations where the peroxy radical concentrations are at or below the detection limit of the MIESR. Moreover, the budget of ozone in the plume as derived from the aircraft measurements in BERLIOZ [Corsmeier et al., 2002] does not allow for much larger formation rates than those calculated from the measured RO2 concentrations and the accepted rate coefficients. Therefore, an unknown oxidation process must exist in the atmosphere for NO. While similar suggestions have been made before [Parrish et al., 1986; Volz-Thomas et al., 1997; Carpenter et al., 1998], the high data quality achieved in PHOEBE precludes the possibility of analytical errors being responsible for the observed discrepancy. Furthermore, the comparison with the ozone budget gives evidence that the unknown process does not lead to a net formation of  $O_3$ . The MIESR data from BERLIOZ and several other campaigns conducted at Schauinsland in southern Germany and at Tenerife suggest that ozone formation rates do not exceed values of 10 ppb/h [Mihelcic et al., 2003].

# 4.3. Model Simulations

#### 4.3.1. Daytime Chemistry

[66] The measurements were used to calculate the radical concentrations with photochemical box models of different complexity, i.e., the Master Chemical Mechanism (MCM) [Jenkin et al., 1997] and the condensed mechanism RACM [Stockwell et al., 1997]. Both models predict the concentrations of OH, HO<sub>2</sub> and RO<sub>2</sub> quite well in the high-NO<sub>x</sub>

regime [Konrad et al., 2003; Mihelcic et al., 2003]. An important conclusion is that the photolysis of HONO accounts for most of the HOx production in these air masses during early morning [Alicke et al., 2003].

- [67] On the other hand, both models significantly overestimate the OH concentrations at low  $NO_x$  (<5 ppb). The disagreement is up to 60% for the MCM and 80% for RACM. The agreement for  $HO_2$  and  $RO_2$  is much better. Ozonolysis of mostly biogenic olefins is an important source of  $RO_2$  and  $HO_2$  in the late afternoon.
- [68] Qualitatively, the results from Pabstthum confirm earlier exercises, in which constrained models were also found to over predict OH concentrations [e.g., Perner et al., 1987; Platt et al., 1988; Poppe et al., 1994; Eisele et al., 1994, 1996; McKeen et al., 1997; Carslaw et al., 1999; George et al., 1999; Hauglustaine et al., 1999; Savage et al., 2001]. The sensitivity studies conducted in PHOEBE demonstrate that missing hydrocarbon reactivity, as argued in several earlier studies, is not the sole reason for the overestimation of OH. This conclusion is possible from the specific RO<sub>2</sub> measurements made in PHOEBE [Mihelcic et al., 2003]. Increasing the VOC reactivity leads to a pronounced over prediction of the RO<sub>2</sub> concentration by the model. The concentrations of all radicals can be brought into reasonable agreement with the measurements when a sink term is introduced in the models, corresponding to a first order loss of approximately 1  $\rm s^{-1}$  for OH or 0.02  $\rm s^{-1}$ for HO<sub>2</sub>, and by increasing the total biogenic VOC reactivity by approximately 20% [Konrad et al., 2003].

#### 4.3.2. Nighttime Chemistry

- [69] The simultaneous observations of NO<sub>3</sub>, RO<sub>2</sub>, HO<sub>2</sub>, and OH during several nights were interpreted with a chemical box model by *Geyer et al.* [2003]. For most of the nights the model results and ambient observations of RO<sub>2</sub> and HO<sub>2</sub> are in good agreement, whereas the modeled OH concentrations are just within the upper limit of the measurements ( $5 \times 10^4$  cm<sup>-3</sup>). In one night (20 and 21 July), when very high mixing ratios of VOCs were encountered, the model yielded a maximum nocturnal OH level of ( $4.1 \pm 0.7$ )  $\times 10^5$  cm<sup>-3</sup>, significantly higher than the measured value of ( $1.60 \pm 0.85$ )  $\times 10^5$  cm<sup>-3</sup>. The overestimation by the model could point to a missing nocturnal sink of OH.
- [70] Reactions of NO<sub>3</sub> with VOCs, mainly with biogenic monoterpenes, were shown to constitute a considerable source of organic peroxy radicals at night.
- [71] Generally a positive linear correlation of the mixing ratios of RO<sub>2</sub> and NO<sub>3</sub> was observed and modeled during the campaign. The model analysis shows that this dependence can be attributed to the role of NO as a sink for both radicals. In addition, the production rate of RO<sub>2</sub> increased with increasing NO<sub>3</sub> concentration during nights, when VOCs were of minor importance for the NO<sub>3</sub> removal. While *Carslaw et al.* [1997] also found a positive correlation of RO<sub>2</sub> and NO<sub>3</sub> at the eastern coast of England, *Mihelcic et al.* [1993] observed a negative correlation for a clean, forested site where the NO<sub>3</sub> losses were dominated by reactions with VOCs.
- [72] The contribution of OH to the nocturnal oxidation of VOCs, CO, and CH<sub>4</sub> was modeled to be 15% of that of NO<sub>3</sub> for the situation at Pabstthum. This corresponds to a contribution of 2.6% by nighttime OH to the 24 hour integral of the total atmospheric oxidation capacity. Since

the model tends to overestimate the measured OH levels at night, the contribution is even smaller and therefore negligible during BERLIOZ.

#### 5. Conclusions

- [73] The measurements made during BERLIOZ at Pabstthum comprise the most complete data set collected so far in the PBL on atmospheric free radicals, as well as the physical parameters and chemical compounds that are thought to control the radical concentrations. Most radicals, i.e., HO<sub>2</sub>, RO<sub>2</sub>, and NO<sub>3</sub>, were measured with two different analytical techniques. The good agreement gives high confidence in the accuracy of the data. The situation is similar for the stable compounds, e.g., excellent agreement (<5%) was observed between four different methods for the measurement of NO<sub>2</sub>, more than 50 hydrocarbons and 30 carbonyl compounds were identified and quantified, and quantitative experimental information was obtained on the relevant photolysis rates that control radical production. For the concentration of HCHO, significant differences of up to a factor of two were observed between DOAS and the in situ measurement, which could not be resolved.
- [74] Although the city plume was observed only for a few hours, the measurements covered the entire range of chemical conditions from continental background (<1 ppb  $NO_x$ ) to suburban air with up to 30 ppb of  $NO_x$ .
- [75] The interpretation of the data set in the accompanying papers leads to important conclusions regarding our understanding of the radical chemistry:
- 1. The NO/NO<sub>2</sub> ratio is 25% lower than predicted by photochemical models and by the PSS approach.
- 2. The photochemical ozone production rate does not seem to exceed values of 10 ppb/h. The production rates derived from PSS are much larger and must be regarded with great caution.
- 3. The large overestimation of OH by the models at low  $NO_x$  mixing ratios suggest a yet unidentified loss process for  $HO_x$  radicals. The  $RO_2$  data show that missing VOC reactivity is not the sole reason.
- 4. Nighttime chemistry initiated by NO<sub>3</sub> radicals and ozonolysis plays an important role in the degradation of many VOCs and is an important source for peroxy radicals at night.
- 5. HONO is an important source for OH in polluted air in the morning.
- [76] Acknowledgments. Many thanks, on behalf of the entire PHOEBE team, to all those who helped during setup and operation of the campaign. Particular thanks go to Angelika and Arthur Schreiner for letting us use their farmland, Andreas Geyer, Frank Holland, Hans Werner Pätz, and Hans-Jürgen Schäfer for their enormous efforts in finding a suitable site for PHOEBE and setting up the necessary infrastructure, Deutsche Telecom for installation of telecommunications, Thomas Heil for installing the computer network and Internet access, and Eberhard Reimer for meteorological forecasts during BERLIOZ and for the climatological data for Berlin-Tempelhof. Hans-Werner Pätz was also a great help in producing of the manuscript. The financial support by the German Minister for Research and Education (BMBF) as part of the Tropospheric Research Focus (TFS, LT 3) is greatly acknowledged.

#### References

Alicke, B., A. Geyer, A. Hofzumahaus, F. Holland, S. Konrad, H.-W. Pätz, A. Schäfer, J. Stutz, A. Volz-Thomas, and U. Platt, OH formation by HONO photolysis during the BERLIOZ experiment, J. Geophys. Res., 108, doi:10.1029/2001JD000579, in press, 2003.

- Armerding, W., et al., Testing the daytime oxidizing capacity of the troposphere: 1994 OH field campaign at the Izana observatory, Tenerife, *J. Geophys. Res.*, 102, 10,603–10,611, 1997.
- Atkinson, R., S. M. Aschmann, W. P. L. Carter, A. M. Winer, and J. N. J. Pitts, Alkyl nitrate formation from the  $NO_x$ -air photooxidations of  $C_2$ – $C_8$  n-alkanes, *J. Phys. Chem.*, 86, 4563–4569, 1982.
- Atkinson, R., W. P. L. Carter, and A. M. Winer, Effects of temperature and pressure on alkyl nitrate yields in the NO<sub>x</sub> photooxidations of n-pentane and n-heptane, J. Phys. Chem., 87, 2012–2018, 1983.
- Atkinson, R., S. M. Aschmann, W. P. L. Carter, A. M. Winer, and J. N. J. Pitts, Formation of alkyl nitrates from the reaction of branched and cyclic alkyl peroxy radicals with NO, *Int. J. Chem. Kinet.*, 16, 1085–1101, 1984.
- Atkinson, R., S. M. Aschmann, and A. M. Winer, Alkyl nitrate formation from the reaction of a series of branched RO<sub>2</sub> radicals with NO as a function of temperature and pressure, J. Atmos. Chem., 5, 91-102, 1987.
- Becker, K. H., and K. Wirtz, Gas phase reactions of alkyl nitrates with hydroxyl radicals under tropospheric conditions in comparison with photolysis, *J. Atmos. Chem.*, 419–433, 1989.
- Becker, K. H., B. Donner, and S. Gäb, BERLIOZ: A field experiment within the German Tropospheric Research Programme (TFS), in *Proceedings of EUROTRAC Symposium 98 Band 2*, pp. 669–672, WIT Press, Southampton, 1999.
- Brandenburger, U., T. Brauers, H.-P. Dorn, M. Hausmann, and D. H. Ehhalt, In-situ measurement of tropospheric hydroxyl radicals by folded long-path laser absorption during the field campaign POPCORN in 1994, *J. Atmos. Chem.*, 31, 181–204, 1998.
- Brauers, T., M. Hausmann, A. Bister, A. Kraus, and H. P. Dorn, OH radicals in the boundary layer of the Atlantic Ocean, 1, Measurements by longpath laser absorption spectroscopy, *J. Geophys. Res.*, 106, 7399–7414, 2001.
- Brune, W. H., et al., Airborne in-situ OH and HO<sub>2</sub> observations in the cloud-free troposphere and lower stratosphere during SUCCESS, *Geophys. Res. Lett.*, 25, 1701–1704, 1998.
- Calvert, J. G., G. Yarwood, and A. M. Dunker, An evaluation of the mechanism of nitrous acid formation in the urban atmosphere, *Res. Chem. Intermed.*, 20, 463–502, 1994.
- Cantrell, C. A., R. E. Shetter, T. M. Gilpin, J. G. Calvert, F. L. Eisele, and D. J. Tanner, Peroxy radical concentrations measured and calculated from trace gas measurements in the Mauna Loa Observatory Photochemistry Experiment 2, J. Geophys. Res., 101, 14,653–14,664, 1996.
- Cantrell, C. A., R. E. Shetter, J. G. Calvert, F. L. Eisele, E. Williams, K. Baumann, W. H. Brune, P. S. Stephens, and J. H. Mather, Peroxy radicals from photostationary state deviations and steady state calculations during the Tropospheric OH Photochemistry Experiment at Idaho Hill, J. Geophys. Res., 102, 6369–6378, 1997.
- Carpenter, L. J., P. S. Monks, I. E. Galbally, C. P. Meyer, B. J. Bandy, and S. A. Penkett, A study of peroxy radicals and ozone photochemistry at coastal sites in the Northern and Southern Hemisphere, *J. Geophys. Res.*, 102, 25,417–25,427, 1997.
- Carpenter, L. J., K. C. Clemitshaw, R. A. Burges, S. A. Penkett, J. N. Cape, and G. G. McFayden, Investigation and evaluation of the NO<sub>x</sub>/O<sub>3</sub> photochemical steady state, *Atmos. Environ.*, *32*, 3353–3365, 1998.
- Carroll, M. A., S. B. Bertman, and P. B. Shepson, Overview of the program for research on oxidants: Photochemistry, Emissions, and Transport (PROPHET) summer 1998 measurements intensive, *J. Geophys. Res.*, 106, 24,275–24,288, 2001.
- Carslaw, N., L. J. Carpenter, J. M. C. Plane, B. J. Allan, R. A. Burgess, K. C. Clemitshaw, H. Coe, and S. A. Penkett, Simultaneous observations of nitrate and peroxy radicals in the marine boundary layer, *J. Geophys. Res.*, 102, 18,917–18,933, 1997.
- Carslaw, N., D. J. Creasey, D. E. Heard, A. C. Lewis, J. B. McQuaid, M. J. Pilling, P. S. Monks, B. J. Bandy, and S. A. Penkett, Modeling OH, HO<sub>2</sub> and RO<sub>2</sub> radicals in the marine boundary layer, 1, Model construction and comparison with field measurements, *J. Geophys. Res.*, 104, 30,241–30,255, 1999.
- Carslaw, N., et al., OH and HO<sub>2</sub> radical chemistry in a forested region of north-western Greece, Atmos. Environ., 35, 4725-4737, 2001.
- Chameides, W., and J. C. G. Walker, A photochemical theory of tropospheric ozone, J. Geophys. Res., 78, 8751–8760, 1973.
- Chameides, W. L., et al., Ozone precursor relationships in the ambient atmosphere, *J. Geophys. Res.*, *97*, 6037–6055, 1992.
- Ciccioli, P., A. Cecinato, E. Brancaleoni, M. Frattoni, and A. Liberti, Use of carbon adsorption traps combined with high resolution gas chromatography-mass spectrometry for the analysis of polar and non-polar C<sub>4</sub>–C<sub>14</sub> hydrocarbons involved in photochemical smog formation, *J. High Resolut. Chromatogr.*, 15, 75–84, 1992.
- Corsmeier, U., et al., Ozone and PAN formation inside and outside of the Berlin plume: Process analysis and numerical process simulations, *J. Atmos. Chem.*, 42, 289–321, 2002.

- Creasey, D. J., D. E. Heard, and J. D. Lee, OH and HO<sub>2</sub> measurements in a forested region of north-western Greece, *Atmos. Environ.*, 35, 4713–4724, 2001
- Crutzen, P. J., The role of NO and NO<sub>2</sub> in the chemistry of the troposphere and stratosphere, *Annu. Rev. Earth Planet. Sci.*, 7, 443–472, 1979.
- Ehhalt, D. H., Photooxidation of trace gases in the troposphere, *Phys. Chem. Chem. Phys.*, 1(24), 5401–5408, 1999.
- Eisele, F. L., G. H. Mount, F. C. Fehsenfeld, J. Harder, E. Marovich, D. D. Parrish, J. Roberts, and T. M. Tanner, Intercomparison of tropospheric OH and ancillary trace gas measurements at Fritz Peak Observatory, Colorado, J. Geophys. Res., 99, 18,605–18,626, 1994.
  Eisele, F. L., D. Tanner, C. A. Cantrell, and J. G. Calvert, Measurements
- Eisele, F. L., D. Tanner, C. A. Cantrell, and J. G. Calvert, Measurements and steady state calculations of OH concentrations at Mauna Loa Observatory, *J. Geophys. Res.*, 101, 14,665–14,679, 1996.
- Eisele, F. L., G. H. Mount, D. Tanner, A. Jefferson, R. Shetter, J. W. Harder, and E. J. Williams, Understanding the production and interconversion of the hydroxyl radical during the Tropospheric OH Photochemistry Experiment, J. Geophys. Res., 102, 6457–6465, 1997.
- Frost, G. J., et al., Photochemical ozone production in the rural southeastern United States during the 1990 Rural Oxidants in the Southern Environment (ROSE) program, *J. Geophys. Res.*, 103, 22,491–22,508, 1998.
- George, L. A., T. Hard, and R. J. O'Brien, Measurements of free radicals OH and HO<sub>2</sub> in Los Angeles smog, *J. Geophys. Res.*, 104, 11,643–11,655, 1999.
- Geyer, A., B. Alicke, D. Mihelcic, J. Stutz, and U. Platt, Comparison of tropospheric NO<sub>3</sub> radical measurements by differential optical absorption spectroscopy and matrix isolation electron spin resonance, *J. Geophys. Res.*, 104, 26,097–26,105, 1999.
- Geyer, A., et al., Nighttime formation of peroxy and hydroxyl radicals during the BERLIOZ campaign: Observations and modeling studies, *J. Geophys. Res.*, 108, doi:10.1029/2001JD000656, in press, 2003.
- Glaser, K., U. Vogt, G. Baumbach, A. Volz-Thomas, and H. Geiss, Vertical profiles of O<sub>3</sub>, NO<sub>2</sub>, NO<sub>x</sub>, VOC and meteorological parameters during the Berlin Ozone Experiment (BERLIOZ) campaign, *J. Geophys. Res.*, 108, doi:10.1029/2002JD002475, in press, 2003.
- Grossmann, D., et al., Hydrogen peroxide, organic peroxides, carbonyl compounds, and organic acids measured in Pabstthum during BERLIOZ, *J. Geophys. Res.*, 108, doi:10.1029/2001JD001096, in press, 2003.
- Harris, G. W., W. P. L. Carter, A. M. Winer, J. N. Pitts, U. Platt, and D. Perner, Observations of nitrous acid in the Los Angeles atmosphere and implications for the predictions of ozone–precursor relationships, *Environ. Sci. Technol.*, 16, 414–419, 1982.
- Harrison, R. M., J. D. Peak, and G. M. Collins, Tropospheric cycle of nitrous acid, J. Geophys. Res., 101, 14,429-14,439, 1996.
- Hauglustaine, D. A., S. Madronich, B. A. Ridley, S. J. Flocke, C. A. Cantrell, F. L. Eisele, R. E. Shetter, D. J. Tanner, P. Ginoux, and E. Atlas, Photochemistry and budget of ozone during the Mauna Loa Observatory Photochemistry Experiment (MLOPEX 2), J. Geophys. Res., 104, 30,275-30,307, 1999.
- Hofzumahaus, A., U. Aschmutat, U. Brandenburger, T. Brauers, H.-P. Dorn, M. Hausmann, M. Heßling, F. Holland, C. Plaß-Dülmer, and D. H. Ehhalt, Intercomparison of tropospheric OH measurements by different laser techniques during the POPCORN campaign 1994, *J. Atmos. Chem.*, 31, 227–246, 1998.
- Holland, F., U. Aschmutat, M. Heßling, A. Hofzumahaus, and D. H. Ehhalt, Highly time resolved measurements of OH during POPCORN using laser-induced fluorescence spectroscopy, *J. Atmos. Chem.*, *31*, 205–225, 1908
- Holland, F., A. Hofzumahaus, J. Schäfer, A. Kraus, and H. W. Pätz, Measurements of OH and HO<sub>2</sub> radical concentrations and photolysis frequencies during BERLIOZ, *J. Geophys. Res.*, 108, doi:10.1029/2001JD001393, in press, 2003.
- Jefferson, A., D. J. Tanner, F. L. Eisele, D. D. Davis, G. Chen, J. Crawford, J. W. Huey, A. L. Torres, and H. Berresheim, OH photochemistry and methane sulfonic acid formation in the coastal Antarctic boundary layer, J. Geophys. Res., 103, 1647–1656, 1998.
- Jeffries, H. E., and S. Tonnesen, A comparison of two photochemical reaction mechanisms using mass balance and process analysis, *Atmos. Environ.*, 28, 2991–3003, 1994.
- Jenkin, M. I., R. A. Cox, and D. J. Williams, Laboratory studies of the kinetics of formation of nitrous acid from the thermal reaction of nitrogen dioxide and water vapour, *Atmos. Environ.*, 22, 487–498, 1988.
- Jenkin, M. E., S. M. Saunders, and M. J. Pilling, The tropospheric degradation of volatile organic compounds: A protocol for mechanism development, *Atmos. Environ.*, 31, 81–104, 1997.
- Junkermann, W., et al., Actinic radiation and photolysis processes in the lower troposphere: Effect of clouds and aerosols, *J. Atmos. Chem.*, 42, 413-441, 2002.
- Kanaya, Y., Y. Sadanaga, J. Matsumoto, U. K. Sharma, Y. Hirokiwa, Y. Kajii, and H. Akimoto, Night-time observation of the HO<sub>2</sub> radical by

- an LIF instrument at Oki Island, Japan, and its possible origins, *Geophys. Res. Lett.*, 26, 2179–2182, 1999.
- Kanaya, Y., Y. Sadanaga, J. Matsumoto, U. K. Sharma, Y. Hirokiwa, and H. Akimoto, Daytime HO<sub>2</sub> concentrations at Oki Island, Japan, in summer 1998: Comparison between measurement and theory, *J. Geophys. Res.*, 105, 24,205–24,222, 2000.
- Kanter, H. J., V. A. Mohnen, A. Volz-Thomas, W. Junkermann, K. Glaser, H. Weitkamp, and F. Slemr, Quality assurance in TSF for inorganic compounds, J. Atmos. Chem., 42, 235–253, 2002.
- Kessler, C., and U. Platt, Nitrous acid in polluted air masses: Source and formation pathways, paper presented at 3rd Symposium on the Physico-Chemical Behavior of Atmospheric Pollutants, Eur. Commun., Varese, Italy, 1984.
- Kibler, M., S. Schlomski, and K. Bächmann, Determination of carbonyl compounds and organic acids in the atmospheric gas-phase and their influence on oxidation capacity, in *Proceedings of EUROTRAC Sympo*sium '98, vol. 1, pp. 350–355, 1999.
- Konrad, S., and A. Volz-Thomas, Characterization of a commercial gas chromatography-flame ionization detection system for the in situ determination of C5-C10 hydrocarbons in ambient air, *J. Chromatogr. A*, 878(2), 215-234, 2000.
- Konrad, S., et al., Hydrocarbon measurements at Pabstthum during the BERLIOZ campaign and modeling of free radicals, *J. Geophys. Res.*, 108, doi:10.1029/2001JD000866, in press, 2003.
- Kraus, A., T. Brauers, D. Brüning, A. Hofzumahaus, F. Rohrer, N. Houben, H.-W. Pätz, and A. Volz-Thomas, Ergebnisse des NO<sub>2</sub>-Photolysefrequenz Meβvergleichs JCOM97, Eine Qualitätssicherungsmaβnahme für das BERLIOZ-Experiment im Rahmen des Förderschwerpunkts Troposphärenforschung Leitthema 3 des BMBF, ICG, Jülich, 1998.
- Kraus, A., F. Rohrer, and A. Hofzumahaus, Intercomparison of NO<sub>2</sub> photolysis frequency measurements by actinic flux spectroradiometry and chemical actinometry during JCOM97, *Geophys. Res. Lett.*, 27, 1115–1118, 2000.
- Kroll, J. H., J. S. Clarke, N. M. Donahue, J. G. Anderson, and K. L. Demerjian, Mechanism of HO<sub>x</sub> formation in the gas-phase ozone–alkene reaction, 1, Direct pressure-dependent measurements of prompt OH yields, J. Phys. Chem. A, 105, 1554, 2001.
- Levy, H., Normal atmosphere: Large radical and formaldehyde concentrations predicted, *Science*, 173, 141, 1971.
- Matsumi, Y., F.-J. Comes, G. Hancock, A. Hofzumahaus, A. J. Hynes, M. Kawasaki, and A. R. Ravishankara, Quantum yields for production of O(1D) in the ultraviolet photolysis of ozone: Recommendation based on evaluation of laboratory data, J. Geophys. Res., 107, 2002.
- Mauldin, R. L., III, G. J. Frost, G. Chen, D. J. Tanner, A. S. H. Prevot, D. D. Davis, and F. L. Eisele, OH measurements during the First Aerosol Characterization Experiment (ACE1): Observations and model comparisons, J. Geophys. Res., 103, 16,173–16,729, 1998.
- McKeen, S. A., et al., Photochemical modeling of hydroxyl and its relationship to other species during the Tropospheric OH Photochemistry Experiment, J. Geophys. Res., 102, 6467–6493, 1997.
- Mihelcic, D., D. Klemp, P. Müsgen, H. W. Pätz, and A. Volz-Thomas, Simultaneous measurements of peroxy and nitrate radicals at Schauinsland, J. Atmos. Chem., 16, 313–335, 1993.
- Mihelcic, D., et al., Peroxy radicals during BERLIOZ at Pabstthum: Measurements, radical budgets, and ozone production, *J. Geophys. Res.*, 108, doi:10.1029/2001JD001014, in press, 2003.
- Moortgat, G. K., et al., Hydrogen peroxide, organic peroxide and carbonyl compounds determined during the BERLIOZ campaign, J. Atmos. Chem., in press, 2002.
- Mount, G. H., and E. J. Williams, An overview of the Tropospheric OH Photochemistry Experiment, Fritz Peak/Ihado Hill, Colorado, fall 1993, *J. Geophys. Res.*, 102, 6171–6186, 1997.
- Müller, M., A. Kraus, and A. Hofzumahaus, Measurements of spectrally resolved actinic fluxes for the determination of tropospheric ozone photolysis frequencies and comparison with data from chemical actinometry, in *First European Symposium on the Effects of Environmental UV-B Radiation*, edited by H. Bauer and C. Nolan, pp. 55–57, 1995.
- Pätz, H.-W., et al., Measurements of trace gases and photolysis frequencies during SLOPE96 and a coarse estimate of the local OH concentration from HNO<sub>3</sub> formation, *J. Geophys. Res.*, 105, 1563–1583, 2000.
- Pätz, H. W., A. Lerner, N. Houben, and A. Volz-Thomas, Charakterisierung eines neuen Verfahrens zur Kalibrierung von Peroxiacetylnitrat (PAN), Schadst. Reinhalt. Luft, 62, 215–219, 2002.
- Parrish, D. D., M. Trainer, E. J. Williams, D. W. Fahey, G. Hübler, C. S. Eubank, S. C. Liu, P. C. Murphy, D. L. Albritton, and F. C. Fehsenfeld, Measurements of the NO<sub>x</sub>-O<sub>3</sub> photostationary state at Niwot Ridge, Colorado, *J. Geophys. Res.*, 91, 5361-5370, 1986.

- Paulson, S. E., and J. J. Orlando, The reactions of ozone with alkenes: An important source of  $HO_x$  in the boundary layer, *Geophys. Res. Lett.*, 23, 3727–3730, 1996.
- Penkett, S. A., P. S. Monks, L. J. Carpenter, K. C. Clemitshaw, G. P. Ayers, R. W. Gillet, I. E. Galbally, and C. P. Meyer, Relationships between ozone photolysis rates and radical concentrations in clean marine air over the Southern Ocean, *J. Geophys. Res.*, 102, 12,805–12,817, 1997.
- Perner, D., et al., Measurements of tropospheric OH concentrations: A comparison of field data with model predictions, *J. Atmos. Chem.*, 5, 185–216, 1987.
- Plass-Dülmer, C., T. Brauers, and J. Rudolph, POPCORN: A field study of photochemistry in north-eastern Germany, *J. Atmos. Chem.*, *31*, 5–31, 1998
- Platt, U., *The Origin of Nitrous and Nitric Acid in the Atmosphere*, edited by W. Jaeschke, pp. 299–319, Springer-Verlag, New York, 1986.
- Platt, U., M. Rateike, W. Junkermann, J. Rudolph, and D. H. Ehhalt, New tropospheric OH measurements, *J. Geophys. Res.*, 93, 5159–5166, 1988.
- Platt, U., G. LeBras, G. Poule, J. P. Burrows, and G. Moortgat, Peroxy radicals from night-time reaction of NO<sub>3</sub> with organic compounds, *Nat-ure*, 348, 147–149, 1990.
- Platt, U., et al., Free radicals and fast photochemistry during BERLIOZ, J. Atmos. Chem., 42, 359–394, 2002.
- Poppe, D., et al., Comparison of measured OH concentrations with model calculations, *J. Geophys. Res.*, 99, 16,633–16,642, 1994.
- Salisbury, G., et al., Production of peroxy radicals at night via reactions of ozone and the nitrate radical in the marine boundary layer, *J. Geophys. Res.*, 106, 12,669–12,687, 2001.
- Savage, N. H., R. M. Harrison, P. S. Monks, and G. Salisbury, Steady-state modelling of hydroxyl radical concentrations at Mace Head during the EASE '97 campaign, May 1997, Atmos. Environ., 35, 515–524, 2001.
- Schlomski, S., M. Kibler, P. Ebert, A. Mainka, T. Prokop, and B. Tenberken, Multiphase chemistry of organic acids and carbonyl compounds, in *Proc. 7th European Symp. Phys. Chem. Behaviour Atmos. Pollutants, Venice 1996*, pp. 557–561, Eur. Commun., Varese, Italy, 1997.
- Siese, M., K. H. Becker, K. J. Brockmann, H. Geiger, A. Hofzumahaus, F. Holland, D. Mihelcic, and K. Wirtz, Direct measurements of OH radicals from ozonolysis of selected alkenes: A EUPHORE simulation chamber study, *Environ. Sci. Technol.*, 35, 4660–4667, 2001.
- Stockwell, W. R., and J. G. Calvert, The mechanism of NO<sub>3</sub> and HONO formation in the night-time chemistry of the urban atmosphere, *J. Geo-phys. Res.*, 88, 6673–6682, 1983.
- Stockwell, W. R., F. Kirchner, M. Kuhn, and S. Seefeld, A new mechanism for regional atmospheric chemistry modeling, *J. Geophys. Res.*, 102, 25,847–25,879, 1997.
- Tan, D., et al., HO<sub>x</sub> budgets in a deciduous forest: Results from the PRO-PHET summer 1998 campaign, *J. Geophys. Res.*, 106, 24,407–24,428, 2001
- Volz-Thomas, A., and B. Kolahgar, On the budget of hydroxyl radicals at Schauinsland during the Schauinsland Ozone Precursor Experiment (SLOPE96), *J. Geophys. Res.*, 105, 1611–1622, 2000.
- Volz-Thomas, A., et al., Photochemical ozone production rates at different TOR sites, in *Tropospheric Ozone Research*, edited by Ø. Hov, pp. 95–110, Springer-Verlag, New York, 1997.
- Volz-Thomas, A., J. Slemr, S. Konrad, T. Schmitz, and V. A. Mohnen, Quality assurance of hydrocarbon measurements in the German Tropospheric Research Focus (TFS), J. Atmos. Chem., 42, 255–279, 2002.
- Volz-Thomas, A., H.-W. Pätz, N. Houben, S. Konrad, D. Mihelcic, T. Klüpfel, and D. Perner, Inorganic trace gases and peroxy radicals during BERLIOZ at Pabstthum: An investigation of the photostationary state of NO<sub>x</sub> and O<sub>3</sub>, J. Geophys. Res., 108, doi:10.1029/2001JD001255, in press, 2003.
- Wayne, R. P., et al., The nitrate radical: Physics, chemistry, and the atmosphere, *Atmos. Environ.*, 25A, 1–203, 1991.
- Wennberg, P. O., et al., Hydrogen radicals, nitrogen radicals, and the production of O<sub>3</sub> in the upper troposphere, *Science*, *279*, 49–53, 1998.
- Winkler, J., et al., Ground-based and airborne measurements of nonmethane hydrocarbons in BERLIOZ: Analysis and selected results, *J. Atmos. Chem.*, 42, 465–492, 2002.
- K.-H. Becker, Fachbereich 9, Physikalische Chemie, Bergische Universität Gesamthochschule Wuppertal, D-42097, Wuppertal, Germany.
   H. Geiß and A. Hofzumahaus, Institut für Chemie und Dynamik der
- H. Geiß and A. Hofzumahaus, Institut für Chemie und Dynamik der Geosphäre II, Forschungszentrum Jülich, D-52425 Jülich, Germany.
- A. Volz-Thomas, Institut für Chemie der Belasteten Atmosphäre (ICG-2), Forschungszentrum Jülich, Leo-Brandt-Straße, D-52425 Jülich, Germany. (a.volz-thomas@fz-juelich.de)

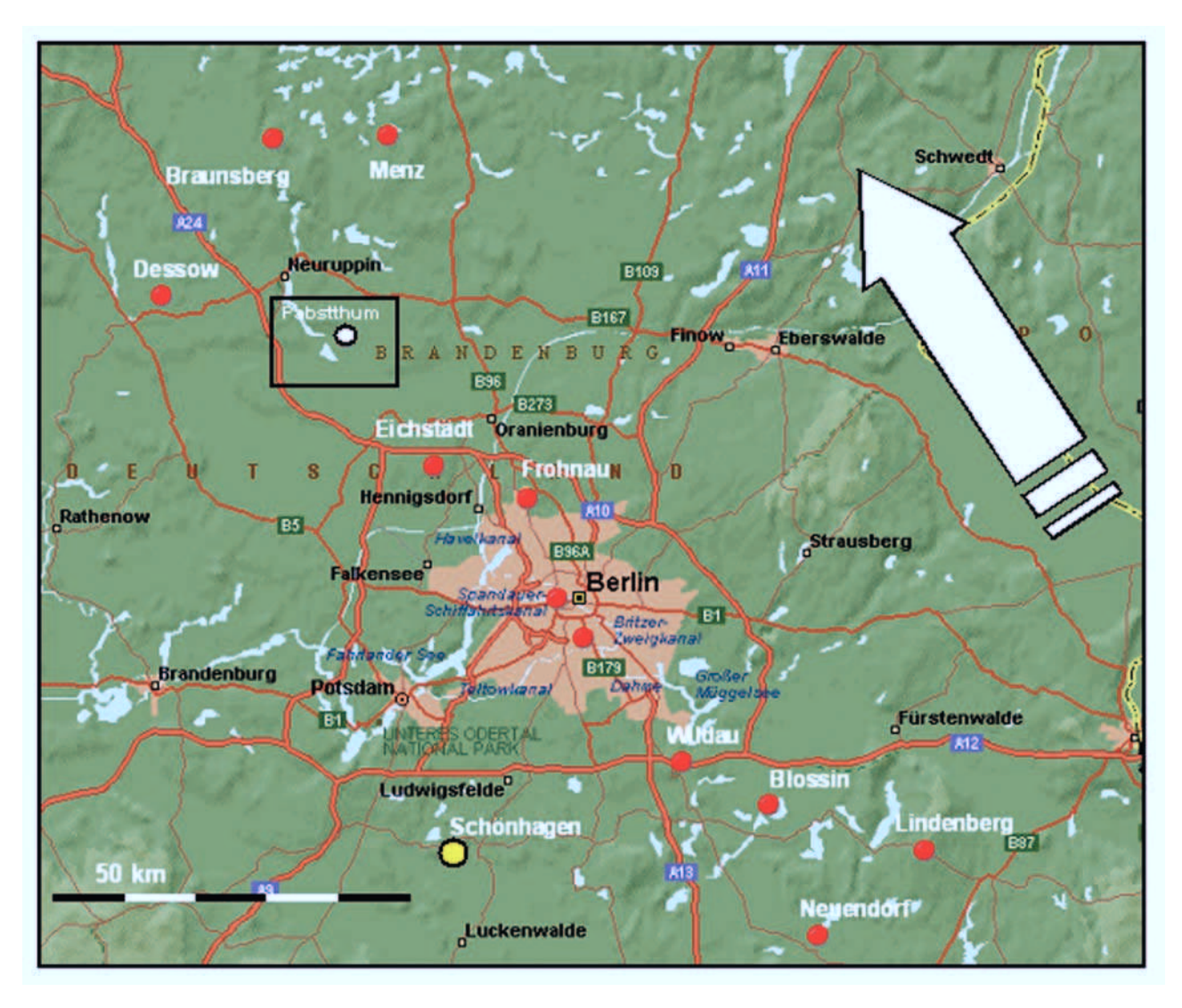


**Figure 1.** Map of the area around Berlin with the surface sites of BERLIOZ indicated by the red dots and the airfield Schönhagen by the yellow dot. The red lines denote motorways and major roads.



**Figure 2.** Surroundings of the PHOEBE observatory site Pabstthum (green: forested areas, blue: water bodies).

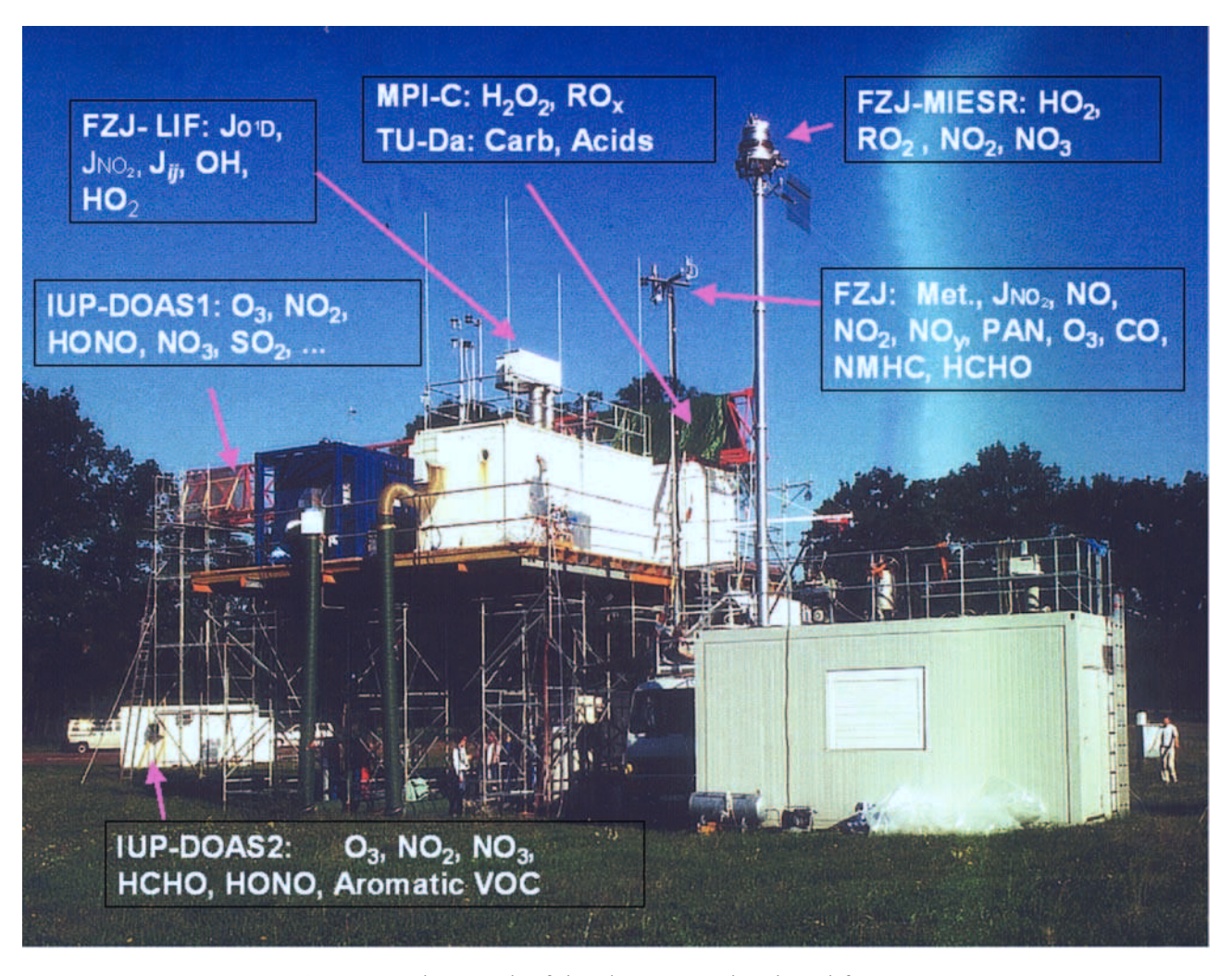
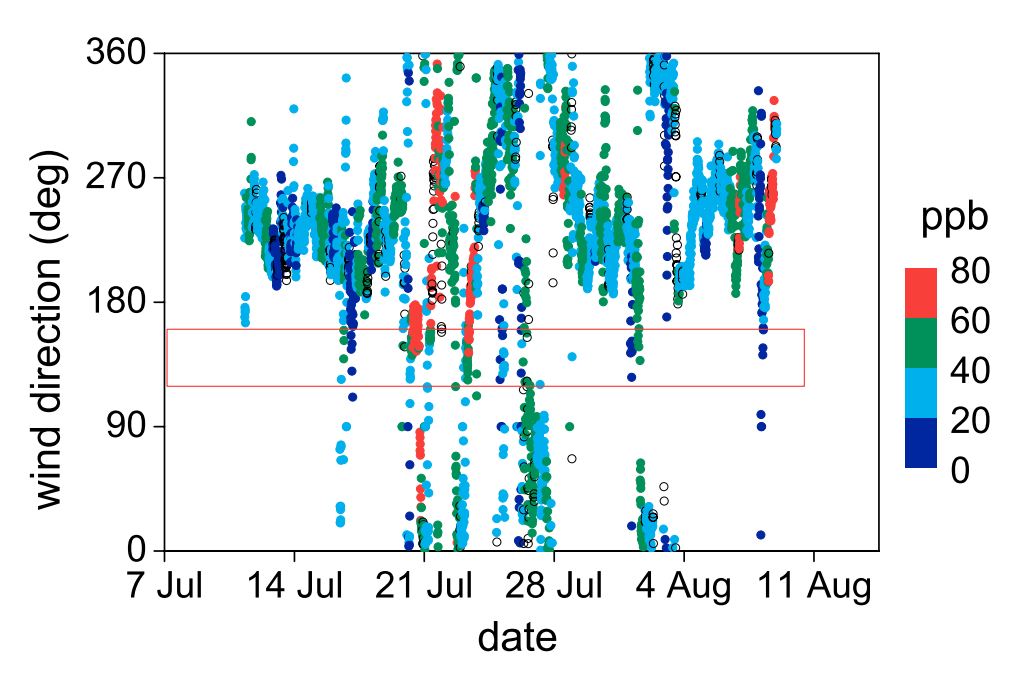
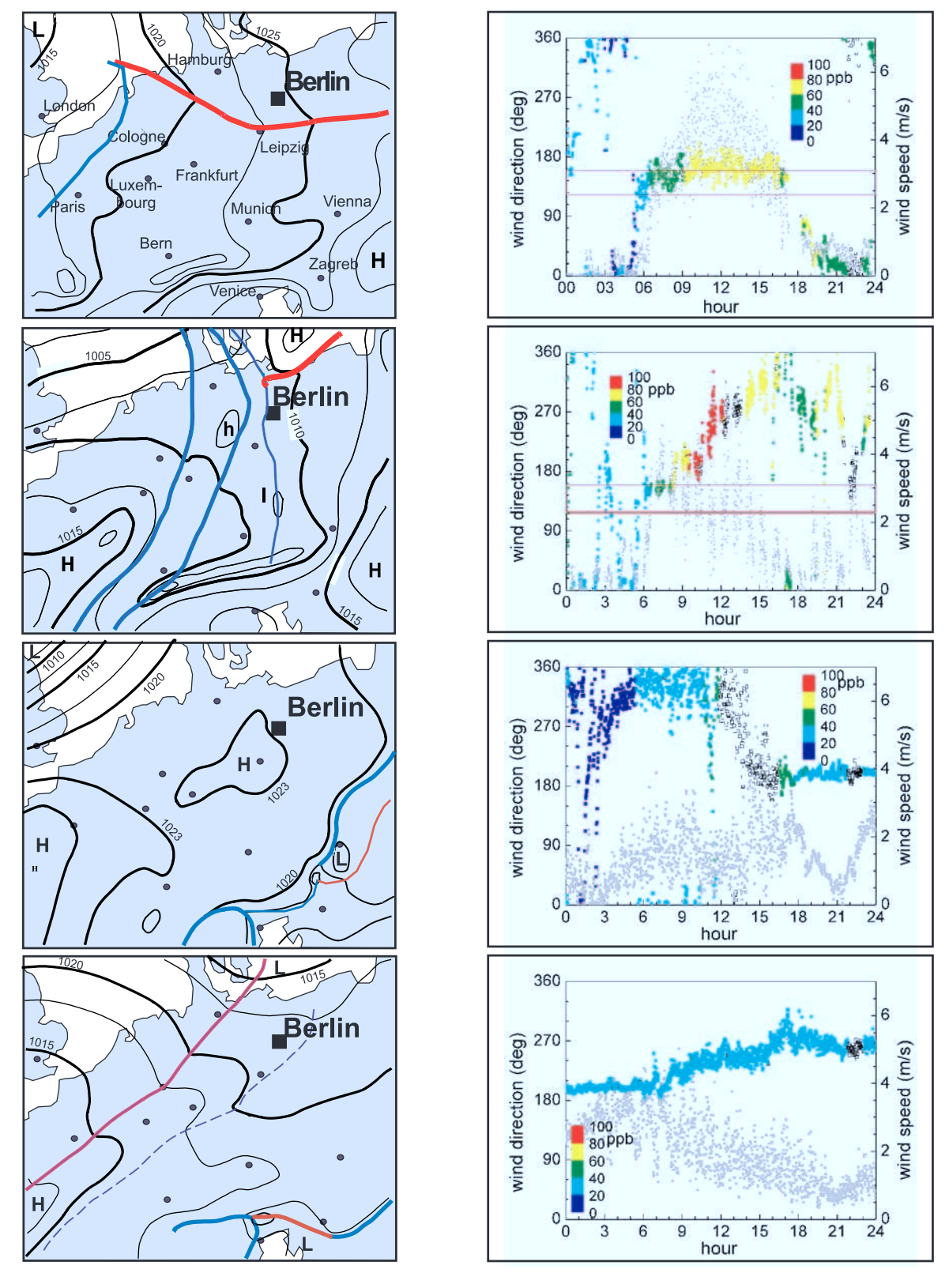


Figure 4. Photograph of the observatory site viewed from east.



**Figure 5.** Time series of the wind direction at Pabstthum during the BERLIOZ campaign (10 min averages). The box indicates the sector for winds coming from the greater Berlin area. Colors denote the  $O_x$  mixing ratio (black circles: missing  $O_x$  values).



**Figure 7.** Meteorological surface charts for 12 UTC (left) and surface wind (at 10 m above ground) at Pabstthum (right) for 20 July (top), 21 July, 3 August, and 4 August (bottom). The color code in the wind direction denotes the  $O_x$  mixing ratio (black circles: missing  $O_x$  values; gray dots: wind speed).